Stream water quality in large glacierized catchments in Central Asia: a perspective on cryosphere and land cover importance

Andrew J Wade[1,*], Vadim Yapiyev[1,2], Maria Shahgedanova[1], Zarina Saidaliyeva[1], Azamat Madibekov[3], Vassiliy Kapitsa[3,4], Nikolay Kasatkin[3,4], Laura Ismukhanova[3], Roza Kulbekova[3], Botakoz Sultanbekova[3], Igor Severskiy[3,4], Mukhammed Esenaman[5], Olga Kalashnikova[5], Ryskul Usubaliev[5], Fakhriddin Akbarov[6], Gulomjon Umirzakov[7], Maksim Petrov[6], Ilkhomiddin Rakhimov[8], Dilorom Kayumova[9], Abdulhamid Kayumov[9]

[1]Department of Geography and Environmental Science, University of Reading, Reading, RG6 6DW, UK

[2]School of Mining and Geosciences, Nazarbayev University, Astana, Kazakhstan

[3]Institute of Geography and Water Safety, Almaty, 050010, Kazakhstan

[4]Central Asia Regional Glaciological Centre under the Auspices of UNESCO, Almaty, Kazakhstan

[5]Central-Asian Institute for Applied Geosciences, Bishkek, Kyrgyzstan

[6]Department of Glaciology and Geology, Institute of Geology and Geophysics, Tashkent, Uzbekistan

[7]National University of Uzbekistan, Tashkent, Uzbekistan

[8]Institute of Water Problems, Hydropower and Environment, Dushanbe, Tajikistan

[9]Centre for Glacier Research of the Academy of Science of the Republic of Tajikistan, Dushanbe, Tajikistan

*Corresponding author: a.j.wade@reading.ac.uk

Keywords: Mountains, semi-arid, urban, nutrients, salinity, endorheic basins, glacial retreat.

Highlights

- Quantification of water quality in glacierized Central Asia catchments (> 485 km^2).
- The cryosphere is a primary and secondary nitrogen source.
- Poor water quality occurs in hot spots rather than being uniformly good or bad.

- Shallow urban groundwater is contaminated by sewage.
- A dilution effect due to melt water was discernable at the lowest monitoring points.

Abstract

This work helps address recent calls for systematic water quality assessment in Central Asia and considers how nutrient and salinity sources, and transport, affect water quality along the continuum from glacier to lowland plain. Spatial and, for the first time, temporal variations in stream water pH, temperature, salinity (electrical conductivity), and nitrate and phosphate concentrations are presented for four catchments (485 – 13 500 km^2), all with glaciers and major urban areas. The catchments studied were: Kaskelen (Kazakhstan), Ala-Archa (Kyrgyzstan), Chirchik (Uzbekistan) and the Kofarnihon (Tajikistan). Measurements were made in cryosphere, stream water, groundwater, reservoir and lake samples over a 22-month period at fortnightly intervals from 35 sites. The results highlight that glacier, permafrost and rock glacier melt were primary and secondary nitrate sources (> 1 mg N l^{-1}) to the headwaters, and there are major increases in salinity and nitrate concentrations where rivers receive inputs from agriculture and settlements. Overall, the water quality complies with national and World Health Organization standards, however there were pollution hot-spots with shallow urban groundwaters contaminated with nitrate (> 11 mg N l^{-1}), and stream salinity above 800 µS cm^{-1} in some agricultural areas. Phosphate concentrations were generally low (< 0.06 mg P l^{-1}) throughout the catchments, and elevated (> 0.2 mg P l^{-1}) only in urban areas due to effluent contamination. A melt-water dilution effect along the main river channels was discernable in the electrical conductivity and nitrate concentration seasonal dynamics, even at the lowest monitoring points. Thus, the input of relatively clean water from cryosphere is an important regulator of main channel water quality in the urban and farmed lowland plains adjacent to the Pamir and Tien Shan, and improved sewage treatment is needed in urban areas.

1. Introduction

Over the past 50 years, glacier retreat has been observed and attributed to climate change, with this trend projected to continue for the next 70 to 100 years (Hock et al., 2019).

Worldwide, approximately 1.9 billion people depend on the water supplied by glaciers for domestic and commercial consumption, irrigation and hydropower, and therefore the assessment of current and future mountain water resources is important (Hock et al., 2019). Outside North America and Europe, relatively little attention has been given to water quality assessment in glacier-fed catchments, and to the relationship with freshwater ecosystems and the provision of clean water for downstream use. In part, this lack of attention on water quality arises because of the practical difficulties and expense of sustained sample collection in remote locations. When done, water chemistry studies of glacierized catchments tend to focus on the spatial and temporal variations in the hydrochemistry with emphasis on water isotopes and the major ions to quantify source water contributions to stream flow, and to assess weathering and the release of potentially toxic elements (Tranter, 2003). Downstream changes in salinity and nutrient concentrations and the seasonal dynamics remain poorly quantified and understood.

Central Asia (CA) is a largely arid region dependent on mountain snow and glacier melt for water supply (Kaser et al., 2010; Viviroli et al., 2020). Model-based estimates of climate-change impacts suggest a glacier-mass reduction, but that glaciers will remain (Farinotti et al., 2015; Hock et al., 2019; Shahgedanova et al., 2020; Shannon et al., 2019; Van Tricht and Huybrechts, 2023). The mass reduction is expected to increase summer flows initially due to increased melt, followed by a summer flow reduction as the melt water declines in the first quarter of this century though the precise timing of 'peak water' remains uncertain (Duethmann et al., 2015; Hagg et al., 2013; Huss and Hock, 2018; Kriegel et al., 2013; Shahgedanova et al., 2020; Shahgedanova et al., 2018). As the catchment headwaters provide water that dilutes downstream contaminant inputs, it is important to assess the salinity and nutrient concentrations from the glacier to the plains to assess potable and irrigation water provision, and eutrophication, along the continuum. As the high mountain cryosphere melts, headwater solute concentrations in the vicinity of the glacier terminus will likely be affected through trace element leaching from the exposed substrate due to weathering, and the release, in meltwater, of legacy pollutants stored in snow, glacier ice, rock glaciers and permafrost (Bogdal et al., 2009; Colombo et al., 2018; Liu et al., 2021). Shifts in the timing of snow and ice melt to earlier in spring and a change precipitation form, from snow to rainfall, are anticipated which will likely

change solute release, including nitrate and phosphate, and stream temperatures (Brahney et al., 2021). Headwater aquatic ecosystems are sensitive to small changes in meltwater hydrochemistry and temperature because of the low stream water concentrations and temperatures. Phosphate, for example, typically has very low stream water concentrations in mountain areas as it is rapidly assimilated by the cryosphere (*e.g.*, cryoconite) and soil and stream biota, and therefore increased concentrations could increase stream and lake productivity (Bettinetti et al., 2008; Bogdal et al., 2009; Colombo et al., 2018; Milner et al., 2017; Miner et al., 2019). Freshly comminuted glacier flour can contain high ion concentrations that can lead to high fluxes with the ion composition dependent on the bedrock. Proglacial streams have been assessed as generally nitrogen limited (Telling et al., 2011; Telling et al., 2012), and increased nitrogen concentrations remain a eutrophication concern given possible nitrogen and phosphorus co-limitation (Jarvie et al., 2018). Downstream, there has been little consideration of lake and reservoir water quality used to supply drinking water and of stream water used for irrigation. The mixing of surface and groundwater has been established as important on the lowland plains around Bishkek with the city almost entirely dependent on an unconfined aquifer fed by precipitation and meltwater for drinking water (Morris et al., 2006). Work is therefore needed to assess aquifer water quality especially given the surface-groundwater interaction.

A recent review of the hydrochemistry and water quality (HWQ) in glacierized CA mountain catchments showed that river water quality mostly complies with national and World Health Organization (WHO) standards, however studies are limited and not all are based on reliable data (Yapiyev et al., 2021). Most publications on CA water quality focus on the middle and lower reaches of the Amu Darya (Crosa et al., 2006) and its main tributary, the Zeravshan (Groll et al., 2015; Olsson et al., 2012) showing that melt water dilutes pollutants released from urban areas and farmland and regulates endorheic lake salinity (Jones and Deocampo, 2003; Orlovsky et al., 2014; Wurtsbaugh et al., 2017). The review also noted that almost no information about hydrochemistry and water quality in CA montane catchments was published after the 1980s and, while the solute chemistry of snow and ice is understood relatively well, only one study was found that described how solutes enter the hydrological system following snow and glacier

ice melt (You et al., 2015). A further recent study assessed nitrogen and phosphorus inputs to the Aral Sea Basin and found that diffuse sources made the greatest contribution to the lower reaches based on two longitudinal sampling campaigns in April and July, 2019 (Leng et al., 2021). Thus, there is a need to build on these works to quantify the extent, dynamics and severity of freshwater contamination in the lowland tributaries draining urban and agricultural areas in CA in different water types, with an emphasis on the importance of the seasonal meltwater dilution effect. Recent papers have highlighted the need for the systematic measurement of contaminants, including nutrients, in CA catchments (Leng et al., 2021; Liu et al., 2021).

The aim of this work is to quantify the influence of the cryosphere on the proglacial zone and downstream stream water quality along the elevation continuum, in lakes and reservoirs in the arid lowlands, and on groundwater in large catchments with major urban centers. Specially, four hypotheses were considered:

1. Weathering, rather than legacy contaminant release from snow and ice melt, is the main nitrate and phosphate source in proglacial streams.
2. Land cover is the predominant control on stream salinity, nitrate and phosphate concentrations, with higher concentrations associated with cropland and urban areas.
3. Urban groundwater is polluted with nitrate and phosphate through mixing with surface waters.
4. Cryosphere melt, during June to August, maintains low stream water salinity, nitrate and phosphate concentrations in the downstream urban and cropland areas.

To achieve the overall aim and test the four hypotheses, fortnightly measurements of pH, water temperature, salinity (electrical conductivity), and nutrient (nitrate, NO_3^--N and phosphate, PO_4^{3-}-P) concentrations were made in surface and groundwater along the elevation continuum to determine the extent of urban and agricultural pollution, and the downstream effect of melt water in the main channel, with samples taken every fortnight for 15-22 months, depending on the site. The analytes were chosen because they are key indicators of water quality overall and could be measured *in situ* or within 24 hours on return from the field to reduce sample

143 degradation effects. The sample collection and analysis were a major logistical effort given
144 catchment areas over 10,000 km^2, altitudes ranging from 200 to over 4000 m.a.s.l., the 2019
145 novel coronavirus (SARS-CoV-2) pandemic, and the large variation in environment including
146 glaciers, alpine grasslands, forests, cropland and dry steppe.

2. Study region

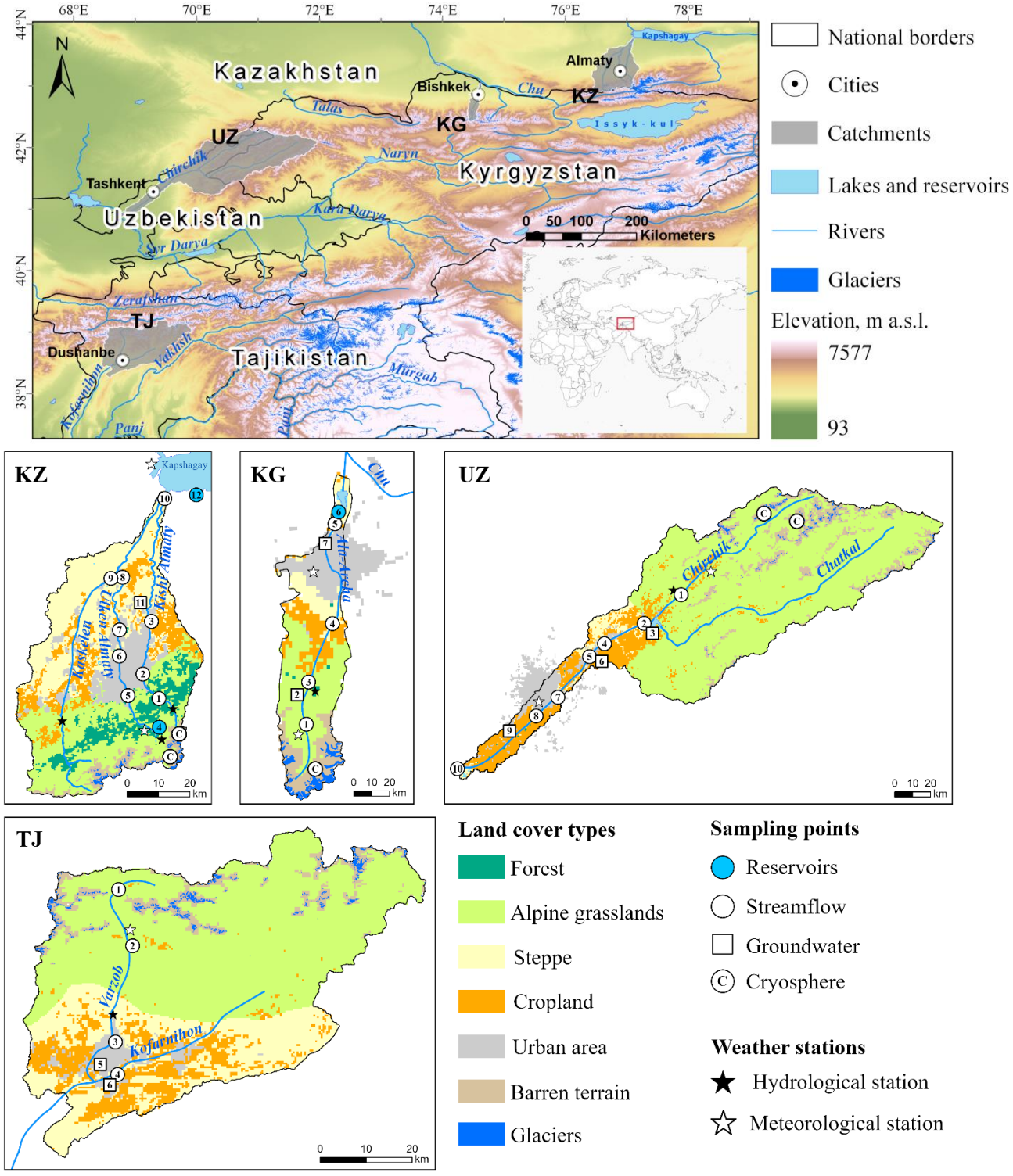

Fig. 1. The study catchments showing the land cover, sample site and weather station locations. The glacierized area shown was derived from the Global Land Ice Measurements from Space (GLIMS) database (Consortium 2017, Raup *et al* 2007). Here and in the subsequent figures: KZ – Kazakhstan, KG – Kyrgyzstan, TJ – Tajikistan, and UZ – Uzbekistan.

Table 1. Study catchment characteristics. The streamflow gauging site locations are shown in Fig. 1. Potential evaporation is from the Climate Research Unit CRU TS 4.01 data set (Harris et al 2014). The glacierized area was calculated for the following years: 2011 (Varzob/Kofarnihon), 2014 (Chirchik), 2017 (all Kazakhstan catchments), 2018 (Ala-Archa). The proportion of the glacierized area is expressed as a percentage of the total catchment area. *The catchment area, glacierized area, elevation range and mean of the Kaskelen catchment includes the Kaskelen River, Ulken Almaty and Kishi Almaty basins.

Country	**Catchment**	**Catchment area (area to upper gauging site)**	**Potential evaporation (1991-2010)**	**Catchment elevation min – max (mean)**	**Glacial area**	**Gauging site name, Lat., Long., (elevation)**	**Discharge (Years)**	**Specific discharge**	**Major city (population)**
		km^2	**mm year^{-1}**	**m.a.s.l.**	**km^2 (%)**	**Decimal degrees (m.a.s.l.)**	**m^3 s^{-1}**	**m^3 s^{-1} km^{-2}**	**million**
Kazakhstan	Kishi Almaty	1048 (43)	900	447 – 4361 (1051)	4.5 (0.4)	Below Sarysai inflow, 43.1396; 77.0684, (1942)	1.5 (2005-2013)	0.034	Almaty (1.78)
	Ulken Almaty	485 (74)		547 – 4355 (2033)	13.8 (2.8)	Upstream of Big Almaty Lake, 43.0389; 76.9947, (2559)	2.3 (2000-2013)	0.031	
	Kaskelen*	3792 (294)		447 – 4361 (1360)	34.0 (0.9)	Kaskelen town, 43.134260, 76.612036, (1129) Kaskelen downstream, 43.7219, 77.0716, (502)	4.0 (2001-2013) 10 (2000-2013)	0.013 NA	
Kyrgyzstan	Ala-Archa	701 (238)	887	608 – 4746 (1940)	31.5 (4.5)	Baityk, 42.647609 74.495405, (1560)	5.5 (1990-2015)	0.019	Bishkek (0.98)
Uzbekistan	Chirchik	13464 (2506)	1129	226 – 4455 (2251)	142.9 (1.1)	Mullala, 41.771928, 70.190761, (925) Chinaz, 40.909312, 68.7593287, (253)	76.9 (1980-2010) 121.9 (2004-2010)	0.031 0.009	Tashkent (2.52)
Tajikistan	Varzob/Kofarnihon	7536 (1275)	1056	673 – 4835 (2170)	98.8 (1.3)	Dagana, 38.702; 68.79, (1056)	50.81 (1990-2011)	0.040	Dushanbe (0.92)

Water quality monitoring was done during 2019 and 2020 in four glacierized catchments in each of Kazakhstan (KZ), Kyrgyzstan (KG), Tajikistan (TJ) and Uzbekistan (UZ, Fig. 1; Table 1). The Kishi Almaty and Ulken Almaty (KZ) are tributaries of the Kaskelen which flows into the Kapshagay reservoir which the Ile river flows into and from. The other three catchments are also the headwaters of major rivers: the Ala-Archa (KG) – of the River Chu; the Chirchik (UZ) – of the Syr Darya, and the Kofarnihon and its tributary, the Varzob (TJ) – of the Amu Darya. All rivers drain large (> 250 km^2) areas and have a glacial-nival regime, and the relative glacial area ranges from 0.4 to 4.5 % of the catchment area. The Kaskelen, Ala-Archa and Chirchik drain from the Tien Shan mountains and the Kofarnihon and Varzob from the Pamir. The Chirchik and Kofarnihon are an order of magnitude larger in area than the Kaskelen and Ala-Archa and longer. All rivers flow through irrigated farmland and cities, with populations of 0.9 – 2.5 million, which rely on river flow, typically stored in mountain reservoirs, for water supply (Table 1). Bishkek in the Ala-Archa basin is an exception as it relies on groundwater almost entirely (Morris et al., 2006) and Dushanbe (TJ) has an approximately even ratio of abstraction from ground and surface water (Finaev et al., 2017). The regional geology and hydrogeology are described in detail elsewhere (Gao et al., 2009; Koronovsky, 2003; Li et al., 2019). In brief, the Tien Shan mountains are comprised of granitoids mainly, and the downstream plains of cropland and dry steppe in the Kaskelen, Ala-Archa and Chirchik are primarily on Quaternary deposits on Meso-Cenozoic sedimentary rocks. The Kofarnihon and Varzob rivers drain from the Devonian volcanic rocks and Carboniferous conglomerates and sandstones of the Pamir, and then also cross Quaternary deposits on Meso-Cenozoic sedimentary rocks. The soils in the four catchments are thin Leptosols in the mountains, and Calcisols around the cities at the mountain base in Kaskelen, Ala-Archa and Chirchik which are characterized by calcium carbonate accumulation. Gleysols occur around Kapchagay in Kaskelen where the soils are wet, and Anthrosols occur in the lowest reaches of the Chirchik near Tashkent modified by farming. In TJ, there are Cambisols in mountain base which are weakly to moderately developed soils, and Anthrosols in the lowest reaches downstream of Dushanbe where the Varzob flows into the Kofarnihon (FAO/IIASA/ISRIC/ISSCAS/JRC, 2012).

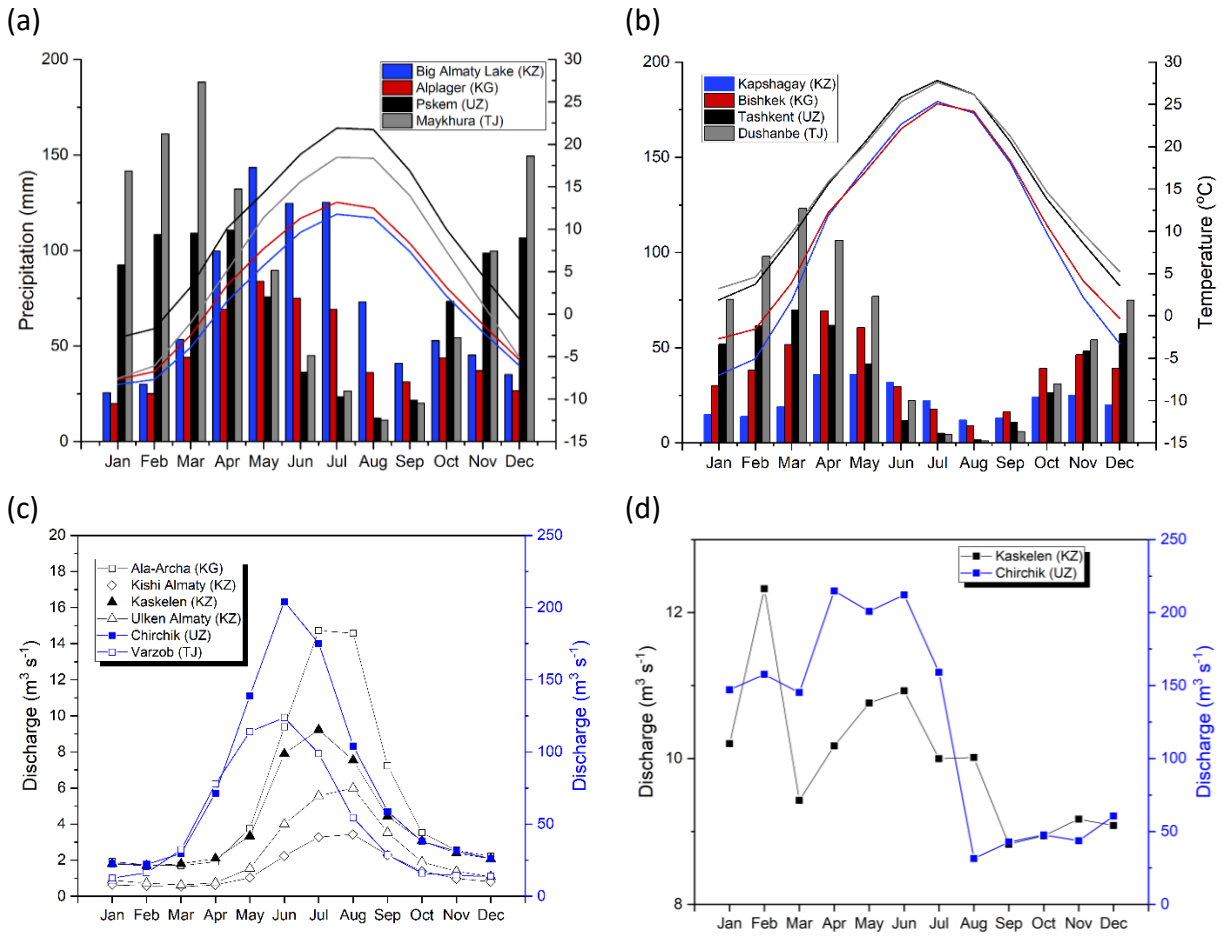

Fig. 2. Air temperature and precipitation at the (a) middle mountain (1200 – 2500 m a.s.l) and (b) plains and foothill (500 – 800 m a.s.l) stations, and streamflow in the (c) middle mountains and on the (d) plains. The blue lines show the catchments in the south and west (UZ, TJ) and the black lines those in the north and north-east (KZ, KG) and the difference between the timing of the peak flow (June in the south and west, July and August in the north and north-east). The meteorological and streamflow gauging site locations are shown in Figure 1. The meteorological data are for the 1980-2020 period if not indicated otherwise and the station elevations are: Big Almaty Lake (2500 m a.s.l.), Alplager (2100 m a.s.l., 1992-2010), Pskem (1256 m a.s.l.), Maykhura (1921 m a.s.l.), Kapshagay (492 m a.s.l, 1971-2000), Bishkek (828 m a.s.l., 1980-2000), Tashkent (488 m a.s.l.), Dushanbe (803 m a.s.l.). The coordinates and elevation of the streamflow gauging sites, and observation period are given in Table 1.

All catchments have large altitudinal gradients in air temperature and precipitation, and distinct seasonal precipitation with a spring maximum (Fig. 2a, b). In the KZ and KG catchments in the north of the region, and in the high mountains, the Köppen climate classification is subarctic and tundra with a humid-continental climate on the lower slopes that transitions to semi-arid grassland steppe (Fig. 1,). In UZ and TJ, to the south, the Köppen climate classification changes

from subarctic in the high mountains to humid-continental and then to a Mediterranean climate as the altitude decreases to semi-arid grasslands and desert. Discharge is an order of magnitude higher in the Chirchik and Varzob which have larger headwater areas than the Ulken Almaty, Kishi Almaty and Ala-Archa though the specific discharge is similar in the Ulken Almaty, Kishi Almaty Chirchik and Varzob (Table 1). The discharge peaks in summer (JJA) in all catchments in the middle mountain sites, although the maximum occurs in June in the south and west (Chirchik, Varzob) compared to July in the north and north-east (Kaskelen, Ulken Almaty, Kishi Almaty and Ala-Archa) catchments and in the catchments where seasonal snowmelt dominates over the runoff from glaciers (Fig. 2c). During winter, in November through to February, stream and river flows are at a minimum.

In this article, *'upland'* or *'high-elevation'* refers to those sites above the transition from forest and alpine grassland to cropland and dry grassland steppe in each catchment (Fig. 1), and *'lowland'* or *'low-elevation'* to the areas downstream of this transition point. *'High-flow'* refers to the surface water flows augmented by glacier and snow melt in JJA (MJJA in Chirchik and Varzob) and *'low-flow'* to the relatively dry-period dominated by baseflow during winter. In the lowlands, the stream flow is heavily modified everywhere except Chon Kyzyl-Suu, with the flows in the lower Kaskelen particularly affected by reservoir storage in the Ulken Almaty and the flows in the lower Chirchik by irrigation abstractions (Fig. 2d). Weathering at the glacial ice-rock interface, is considered a *primary* source of ions, whilst legacy ion release from snow and glacial ice is considered a *secondary* source with, in the case, the primary source distant and the material transported to the cryosphere through the atmosphere and deposited (Chen et al., 2022; Painter et al., 2012).

3. Materials and methods

3.1. Surface and groundwater samples

Once every two weeks for 22 months, water samples were collected at fixed locations along the main channel from the periglacial headwaters to the lowlands, from large tributaries, and from three deep wells, two wells that were artesian and three springs to characterize the

groundwater water chemistry (Fig. 1, Table 2). The samples were analyzed for NO_3^--N, and PO_4^{3-}-P and dissolved Fe concentrations (section 3.3). Sample collection started between April and July 2019 and ended between October 2020 and January 2021 dependent on the country (Table 2). The water was sampled using a plastic syringe and filtered through a 0.45µm syringe filter (Fisher Scientific, part No. 15216869) in the field into a 30 ml universal plastic screw cap tube. The samples were stored in a portable fridge and analyzed in a laboratory within 24 hours at room temperature. Water temperature, electrical conductivity (EC), pH and total dissolved solids (TDS) were measured in the field using a hand-held field meter (Hanna Instruments Inc, model HI 9812-5) and combination probe (Hanna Instruments Inc, model HI 1285-5). The portable meters were calibrated before each day of sampling. The sampling locations were chosen to represent different land uses, the headwater to lowland continuum, and the main water sources: glacial headwaters, main channel and tributaries, groundwater, lakes and reservoirs (Fig. 1; Table 3). The TDS measurements, which are derived from the EC data, did not compare well with ion balances made using major cation and anions measured in a companion hydrochemistry study, and further investigation of the TDS data is needed and therefore it is not reported here. The cold water temperatures meant that water samples had to be returned to the laboratory for nitrate and phosphate analysis; *in situ* measurement, to minimize sample degradation, using portable spectrophotometers was not possible as the samples were too cold for analysis.

3.2. Cryosphere samples

Snow and glacial melt water samples were collected during the summers of 2019 and 2021 at the Tuyuksu (KZ) and Golubin (KG) glaciers, and at the Barkrak and Tekesh glaciers (UZ) in 2020 (see Table S2 for detailed cryosphere sampling sites information, Fig. 1). Sampling in TJ in 2020 was prevented by Covid-19 travel restrictions. The snow samples were collected from snow pits using plastic scoops, placed in plastic bags, melted at room temperature, and filtered and stored as the other water samples. The snow pit sampling was most extensive in KZ where, in 2019, samples were collected from 6 cm layers from the top to the bottom of the snow pit (See Table S2). In 2020, the snow pit was divided into three equal vertical layers of the overall depth

of 162 cm and one sample was taken from each layer (see Table 2, Table S2). In Kyrgyzstan, the cryosphere samples (snow, glacial ice and glacial melt) were collected in 2019 and 2020 (see Table S2). In Uzbekistan, 13 cryosphere samples were collected from the Tekesh and Barkrak glaciers in June and July 2020 (Table 2, Table S2). In Kazakhstan, at least three glacial melt-water samples were collected in immediate proximity of the Tuyuksu glacier terminus. Water samples were also collected from the Gorodetskiy and Morennyi rock glaciers and melting permafrost in the Ulken and Kishi Almaty headwaters. In total cryosphere samples were taken at 39 unique locations, and the pH, EC and water temperature were measured *in situ* except were samples required melting, and NO_3^--N and PO_4^{3-}-P was measured on return to the laboratory. Not all analytes could be measured in every sample (see Table S2 for details and data).

Table 2.

A summary of the sampling program. Kaskelen includes the Ulken and Kishi Almaty sub-catchments.

Catchment	**Kaskelen (KZ)**	**Ala-Archa (KG)**	**Chirchik (UZ)**	**Varzob/ Kafornihon (TJ)**
Fortnightly stream water sampling (n=812)				
Sample type	Monitoring period and number of samples (n)			
Stream water	April 2019 to January 2021 (n=410)	June 2019 to December 2020 (n=135)	June 2019 to November 2020 (n=153)	July 2019 to September 2020 (n=114)
Cryosphere sampling (n=128)				
Mountain snow	June 2019, May 2020 and 2021 (n=70)	August 2019 and 2020 (n=2)	July and August 2020 (n=3)	NA
Glacier melt	August 2019, August and September 2020, August 2021 (n=16)	August 2019 and 2020 (n=4)	July and August 2020 (n=6)	NA

Permafrost melt	August and September 2020, August 2021 (n=7)	NA	NA	NA
Rock glacier melt	August and September 2020, August 2021 (n=7)	NA	August 2020 (n=2)	NA
Proglacial streams	August 2019, September 2020, August 2021 (n=8)	NA	July and August 2020 (n=3)	NA

276

277 *3.3 Laboratory analysis*

278 Nitrate and phosphate concentrations were measured using a laboratory spectrophotometer
279 (Hach Lange Ltd., model DR3900) and the manufacturer's reagent kits: nitrate cuvette test (part
280 Nr. LCK 339), phosphate ortho/total cuvette test (part Nr. LCK 349) and iron trace cuvette test
281 (part Nr. LCK521). Calibration of the spectrophotometer was checked using manufacturer
282 standards (part Nr. LCA 721) before each analysis using a one-point calibration. Every two
283 months, a set of three standard solutions for each analyte was prepared to check calibration
284 drift with a ±10% deviation considered acceptable. Nitrate and phosphate concentrations were
285 reported in mg l^{-1} of NO_3^--N and PO_4^{3-}-P. The detection limits were 0.23 mg N l^{-1}, 0.05 mg P l^{-1}
286 and 0.01 mg Fe l^{-1}. Dissolved iron concentrations were found to be very close to, or below, the
287 limit of detection at all sites, and therefore dissolved iron measurement was stopped after six
288 months given cuvette and standard costs.

289

290 *3.4 Land cover, glacial area and potential evaporation*

291 The Moderate Resolution Imaging Spectroradiometer (MODIS) Land cover product (MCD12Q1,
292 Type 1) was used for land cover classification of the study catchments with a 500 m pixel
293 resolution (Friedl and Sulla-Menashe, 2019). The product, using 2018 imagery, identified 17
294 land cover classes of which 13 were present and merged as follows for use in this study: forest
295 (class 1-9); grasslands (10-11), and croplands (12 and 14) (see Supplementary Material Table 1).
296 Grasslands were divided into alpine grasslands and steppe based on elevation. Land cover area
297 was calculated for each sub-catchment using the 'Calculate geometry' function in ArcGIS Pro,

and the sub-catchment boundary was delineated using the Spatial Analyst Hydrology tool using the sampling point as the pour point. Glacier extent was delineated using the semi-automated glacier mapping method using Landsat 5 and 8 TM and Sentinel 1 and 2 imagery (Narama et al., 2010; Severskiy et al., 2016). CRU potential evapotranspiration (PET) data were obtained for 1991-2010 (grid resolution 0.5°; CRU TS v. 4.03) (Harris et al., 2020).

3.5 Statistical methods

The differences between cryosphere melt measurements for each catchment were visualized using stacked box and whisker diagrams (Fig. 3) with one-way ANOVA done on the means using parametric (Welch) and non-parametric (Kruskal-Wallis) tests (R package: ggstatplot, Supplementary material, Fig. S1). The spatial variations in the surface water and groundwater quality mean values were plotted with the land cover as a background for initial visual inspection (Figs. 4 and 5) and summary statistics calculated for each site (Table 1). The differences between the upland and lowland surface water and groundwater for each catchment were also visualized using stacked box and whisker diagrams (Fig. 6) with one-way ANOVA done using the same methods as used with the cryosphere measurements (Supplementary material, Fig. S2). Paired scatterplots were drawn and the Spearman's correlation co-efficient and the associated significance calculated to determine the correlation between analytes and with land cover using all data (Fig. 7a) and by catchment (Fig. 7b) to test the strength and significance of the correlations. Many of the sample sites were located on the same tributaries and therefore data from the same channel are autocorrelated and dependent. For this reason, no regression analysis was done and two land cover types only, cropland and urban, are shown and discussed because of the high, negative correlation between these and the land covers associated with the uplands: glaciers, barren terrain, forests and alpine grassland.

4. Results and Discussion

4.1. Cryosphere water quality

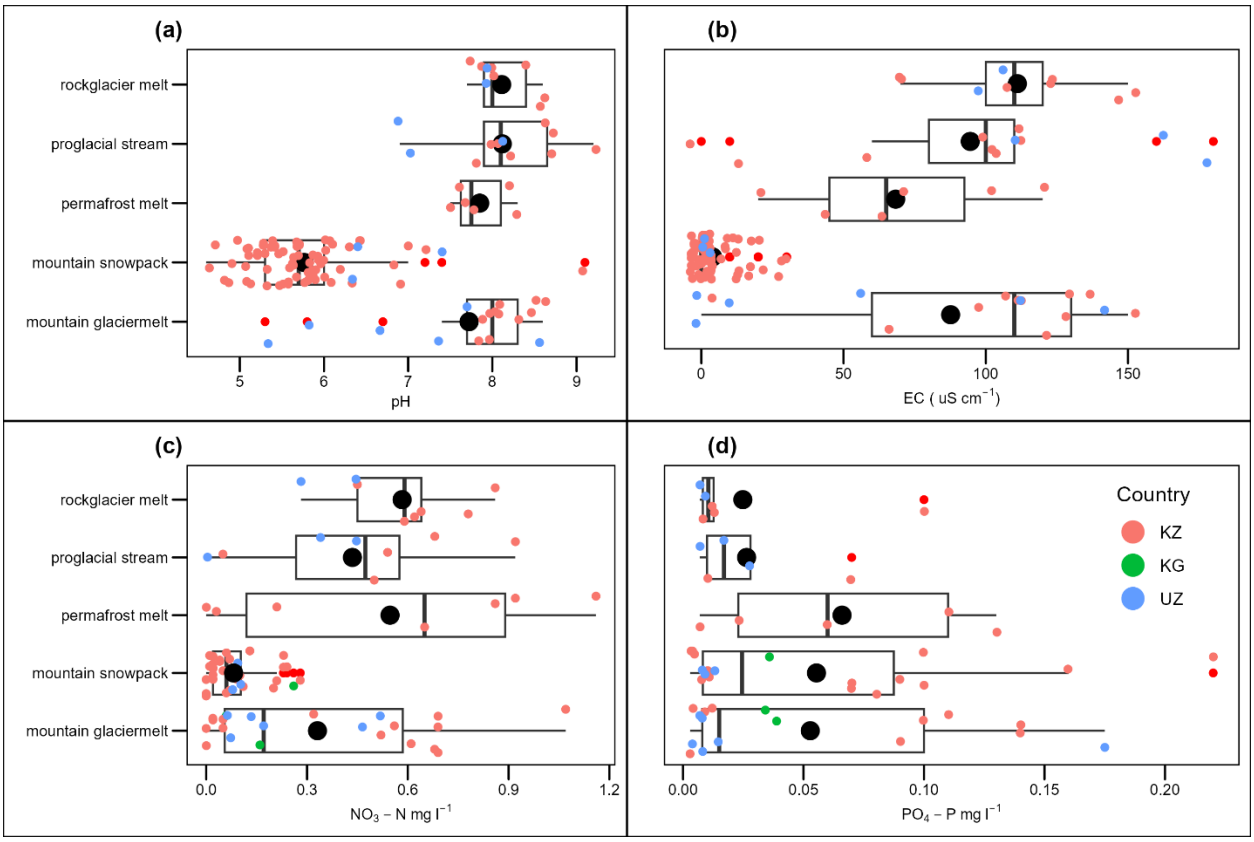

Fig. 3. Cryosphere water quality: (a) pH, (b) EC, (c) NO_3^--N and (d) PO_4^{3-}-P in rock glacier melt, proglacial streams, permafrost melt, mountain snowpack and mountain glacier melt. Black points are mean values and red values are extremes. Parametric and non-parametric ANOVA tests are presented in the Supplementary Material.

The water quality (pH, EC, NO_3^--N and PO_4^{3-}-P) of the cryosphere samples, rock glacier melt, permafrost melt, mountain snowpack, glacier melt and proglacial stream water, is presented in Figure 3. The mountain snowpack was acidic with a mean pH of 5.8, which was significantly lower than the mean pH for the glacier, proglacial stream, permafrost and rock glacier melt (Fig. 3a, Welch, $\rho < 0.001$, See Supplementary Materials for full details). The lower snow pH reflects the interaction between precipitation and atmospheric carbon dioxide, and sulphur and nitrogen oxides, to form weak carbonic acid and sulphuric and nitric acids, and the further absorption of carbon dioxide during snow melt. In contrast, other melt and proglacial stream waters were neutral or slightly alkaline with a mean pH of 7.3, 7.6 and 8.1 for permafrost, rock glacier and glacier melt respectively, and 8.1 for the proglacial streams; all indicative of greater contact with soil and bedrock, which likely contain carbonates mostly as $CaCO_3$ (Fig. 3a)

(Yapiyev et al., 2021). Three glacial melt samples were acidic, reaching as low as 5.4, which was attributed to fresh snow melt.

The EC of the cryosphere samples was lowest for the mountain snowpack (n = 73) with a mean of approximately 4 µS cm^{-1} and varied most in glacier melt (n = 17) from zero to 150 µS cm^{-1} (with mean and median values of 90 and 120 µS cm^{-1}) (Fig. 3b). Rock glacier (n = 9) and permafrost melt (n = 6) were relatively rich in ions with a mean EC of approximately 110 and 70 µS cm^{-1}, respectively, again likely due to greater rock: water ratios and rock-water contact times. The rock glacier and permafrost melt had higher mean nitrate concentrations (*c.* 0.5 - 0.6 mg N l^{-1}) compared to glacier melt, though the glacier melt nitrate concentrations were highly variable, ranging from zero to 1.16 mg N l^{-1} (Fig. 3c). Mountain snowpack nitrate concentrations were lowest among all the cryosphere samples with a mean value of 0.1 mg N l^{-1}. The nitrate concentrations measured in the glacier melt, permafrost melt and the proglacial streams were all highly variable, and only the mean nitrate concentrations in the rock glacier melt were significantly higher ($\rho < 0.01$) than those in the snow melt when using the parametric Welch test. Using the non-parameter Kruskal-Wallis test, all melt and proglacial stream nitrate concentrations were significantly higher ($\rho \leq 0.05$) than those in snow melt. The large variation in the proglacial stream nitrate and EC concentrations suggests mixing at the glacier terminus of nitrate derived from basal debris and rock weathering, a primary nitrate source, and nitrate derived from the release of legacy wet and dry nitrate deposition stored in snow, a secondary nitrate source. The cryosphere phosphate concentrations were all low with means of approximately 0.05 ± 0.03 mg P l^{-1} which was close to the detection limit. The highest phosphate concentrations observed in the mountain snowpack and glacier melt with a maximum concentration of 0.22 mg P l^{-1} in the Tuyuksu snow melt (Fig. 3d). No significant differences between group means were identified. This suggests less distinction between the phosphate concentrations in wet and dry deposition and those derived from melt water contact with rock and basal debris, with any available phosphate rapidly taken up by the biota (Darcy and Schmidt, 2016; McCutcheon et al., 2021).

369 (a) (b)

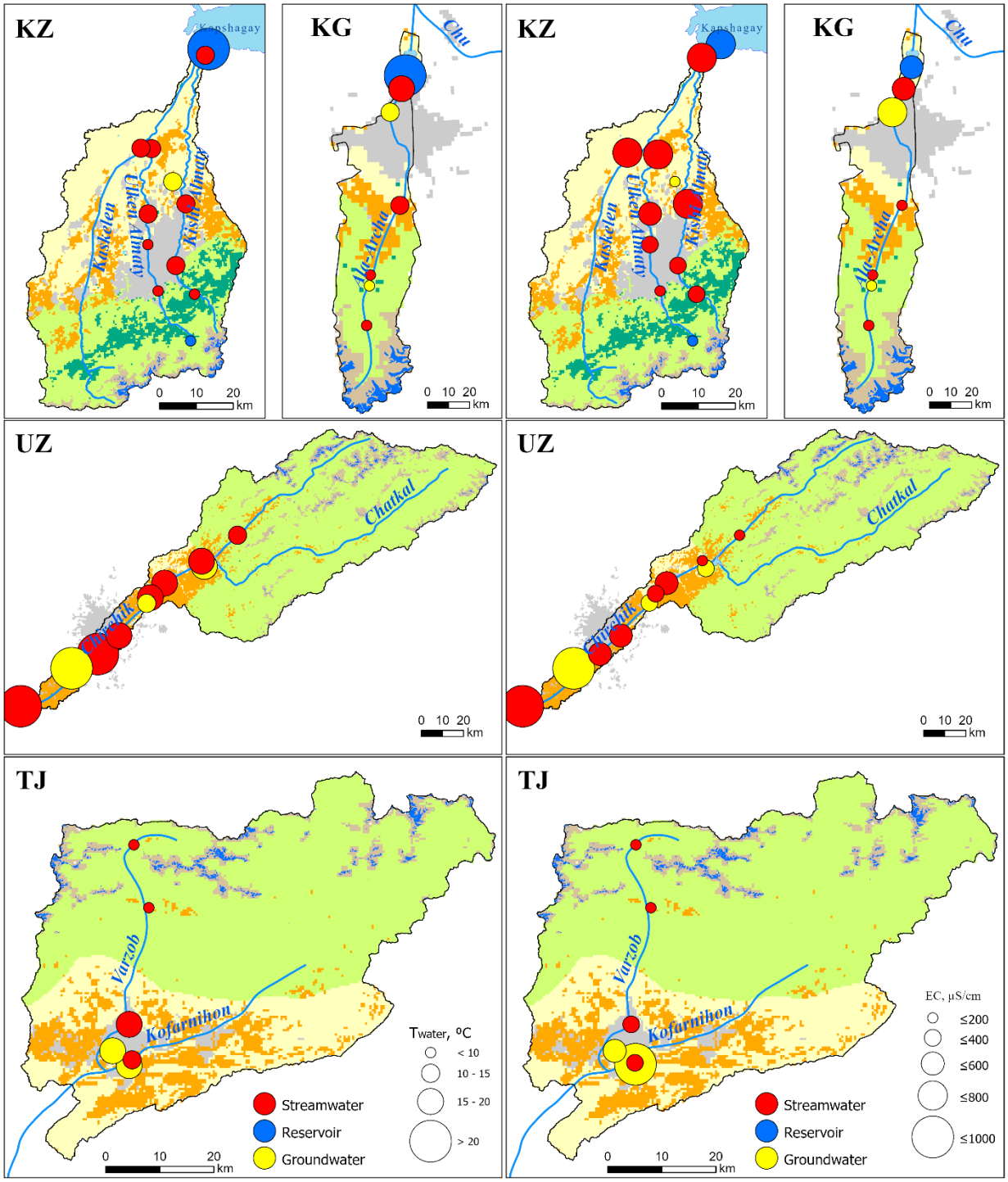

370

371 Fig. 4 Stream water, reservoir and groundwater mean (a) water temperature and (b) EC concentrations.

372 The background shading shows the land cover classes as defined in Fig. 1.

373

374

375 (a) (b)

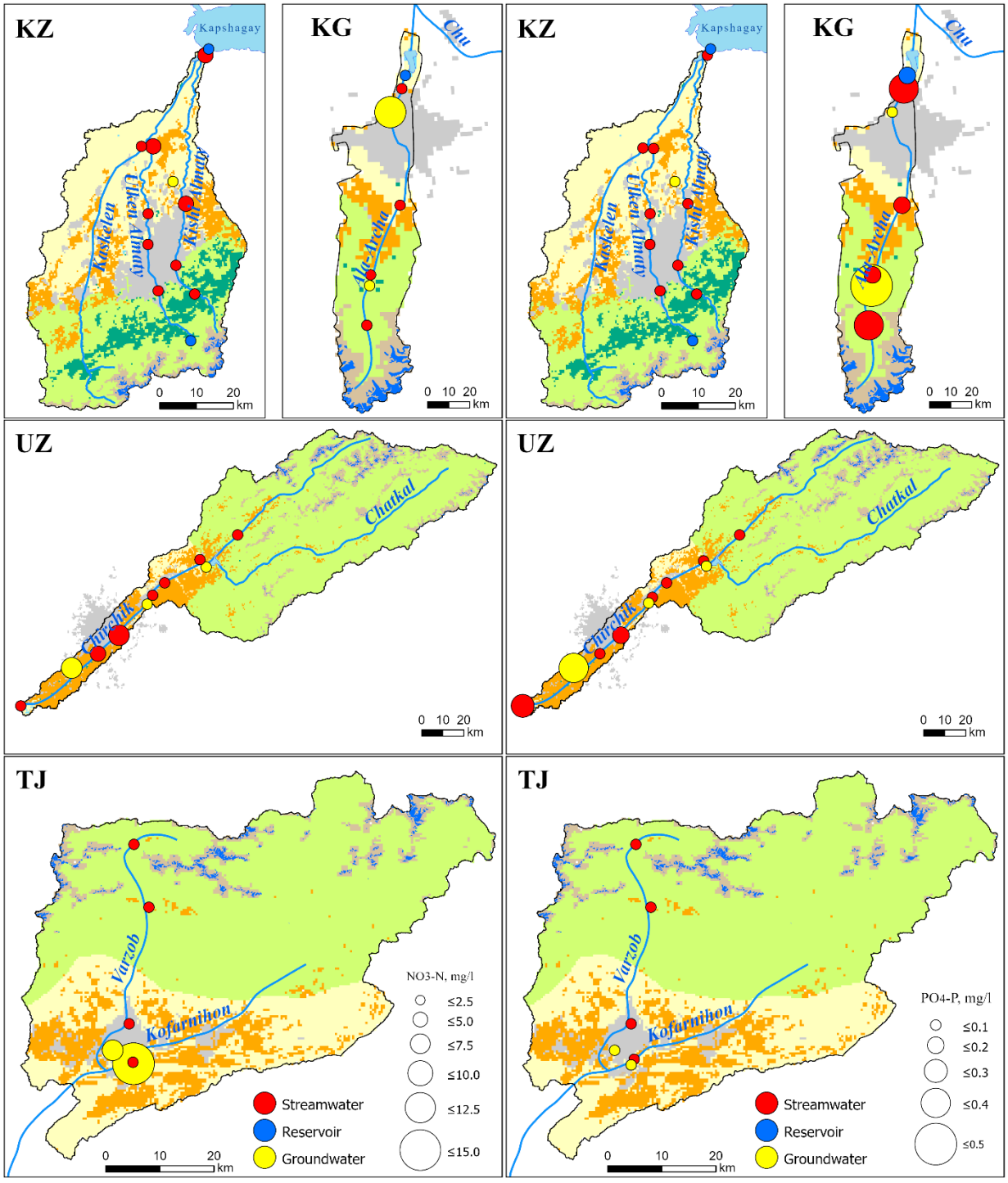

376

377 Fig. 5. Stream water, reservoir and groundwater mean (a) NO_3^--N and (b) PO_4^{3-}-P concentrations. The

378 background shading shows the land cover classes as defined in Fig. 1.

Table 3. Stream water quality descriptive statistics (mean, maximum and minimum): water temperature (ºC), pH, EC (µS cm^{-1}), pH, NO_3^--N (mg l^{-1}), PO_4^{3-}-P (mg l^{-1}). The detection limits were 0.23 mg N l^{-1} and 0.05 mg P l^{-1} and therefore many phosphate measurements were below detection. Abbreviations: Elev. = elevation (m.a.s.l), Ground = groundwater, us = upstream, ds = downstream, gs = gauging station.

							Mean					Max					Min				
Location	**Site code**	**Lat, N**	**Lon, E**	**Elev. (m)**	**Sample type**	**n**	T (ºC)	pH	EC (µS cm^{-1})	NO_3^--N (mg l^{-1})	PO_4^{3-}-P (mg l^{-1})	T (ºC)	pH	EC (µS cm^{-1})	NO_3^--N (mg l^{-1})	PO_4^{3-}-P (mg l^{-1})	T (ºC)	pH	EC (µS cm^{-1})	NO_3^--N (mg l^{-1})	PO_4^{3-}-P (mg l^{-1})
Kishi Almaty, us	KZ-1	43.174	77.015	1333	Stream	38	5.7	8.0	201	0.95	0.009	15	8.4	290	1.20	0.021	0.0	7.6	140	0.68	0.000
Kishi Almaty, Almaty	KZ-2	43.251	76.959	826	Stream	18	12.3	8.2	212	1.08	0.018	20	8.5	350	4.02	0.129	3.0	7.6	150	0.59	0.003
Otegen Batyr	KZ-3	43.406	77.015	628	Stream	38	11.1	8.2	725	4.11	0.067	24	8.6	990	6.39	1.660	1.0	8.0	540	0.93	0.000
Big Almaty Lake	KZ-4	43.057	76.986	2516	reservoir	40	4.9	8.1	133	0.65	0.006	10	8.5	220	0.95	0.033	0.0	7.7	90	0.54	0.000
First President Park	KZ-5	43.192	76.890	993	Stream	38	5.9	8.0	174	0.72	0.008	19	8.6	310	1.31	0.016	0.0	7.6	130	0.20	0.000
Darhan	KZ-6	43.312	76.870	700	Stream	40	8.1	8.0	328	1.60	0.007	18	8.4	750	3.45	0.029	0.0	7.7	170	0.69	0.000
Kazcik	KZ-7	43.390	76.881	658	Stream	40	10.2	8.1	440	2.36	0.009	20	8.9	720	5.28	0.033	0.0	7.6	200	0.77	0.000
Kosozen, Ulken Almaty	KZ-8	43.561	76.908	558	Stream	38	12.1	8.2	616	3.28	0.009	26	8.5	1530	5.46	0.026	0.0	7.8	280	1.45	0.000
Kaskelen	KZ-9	43.562	76.898	558	Stream	38	12.1	8.3	613	1.88	0.045	23	8.5	780	3.14	0.278	0.0	8.0	460	0.54	0.000
Arna village	KZ-10	43.778	77.134	482	Stream	40	13.0	8.3	667	2.54	0.045	26	8.6	810	4.24	0.152	0.0	7.8	370	0.36	0.002
AgroBioCenter	KZ-11	43.466	76.978	609	Ground (artesian)	37	13.4	8.2	198	0.65	0.019	22	8.8	290	1.74	0.028	12.0	7.8	160	0.51	0.004
Kapshagay	KZ-12	43.794	77.147	476	Reservoir	5	21.8	8.4	740	0.33	0.005	26	9	960	1.16	0.010	10.0	8.0	470	0.03	0.002
Alplager	KG-1	42.565	74.480	2135	Stream	26	7.7	7.6	72	0.68	0.381	13	8.3	190	1.23	2.730	3.0	6.7	30	0.05	0.003
Spring, Ala Archa	KG-2	42.630	74.491	1690	Ground (spring)	15	7.7	8.0	a	0.67	0.421	16	8.1	240	0.90	1.860	2.0	7.9	130	0.08	0.006
Baityk	KG-3	42.648	74.495	1589	Stream	29	7.6	7.7	109	0.63	0.165	16	8	280	1.18	0.741	2.0	7.2	50	0.01	0.000
Zarechnoe	KG-4	42.759	74.571	1080	Stream	28	11.4	7.8	132	0.66	0.109	26	8.1	220	2.46	0.633	1.0	7.3	16	0.00	0.004
Bridge	KG-5	42.950	74.592	663	Stream	29	15.4	8.0	481	2.05	0.316	28	8.4	790	4.01	3.010	4.0	7.3	240	0.04	0.001
Ala Archa reservoir	KG-6	42.971	74.602	660	Reservoir	6	21.8	8.0	558	1.74	0.191	29	8.5	720	3.12	0.390	14.0	7.4	360	0.39	0.022

Household well	KG-7	42.913	74.563	702	Ground (urban)	2	13.0	7.3	655	11.20	0.058	13	7.3	680	11.20	0.098	13.0	7.3	630	11.20	0.017
Pskem, Mulala	UZ-1	41.772	70.191	929	Stream	18	10.3	8.2	166	0.50	0.017	17	8.6	220	0.64	0.056	0.6	8.1	130	0.42	0.001
Chirchik, ds Charvak reservoir	UZ-2	41.630	69.953	748	Stream	18	15.2	8.3	178	0.47	0.094	20	8.8	240	0.70	0.707	5.0	8.0	130	0.36	0.005
Hodjakent	UZ-3	41.623	69.940	769	Ground (spring)	18	16.0	8.2	256	1.43	0.030	29	8.4	290	6.73	0.107	9.0	7.9	200	0.97	0.008
Chirchik, ds Gazalkent	UZ-4	41.530	69.688	636	Stream	18	17.3	8.1	449	2.16	0.050	23	8.4	640	3.58	0.290	5.0	7.6	150	0.81	0.004
Chirchik	UZ-5	41.431	69.583	561	Stream	18	17.2	8.3	268	0.93	0.058	22	8.5	450	1.76	0.304	8.0	8.1	180	0.56	0.000
Spring, Chirchik	UZ-6	41.431	69.583	561	Ground (spring)	10	15.0	7.6	355	1.68	0.050	20	7.7	410	1.92	0.277	11.0	7.5	290	1.41	0.010
Chirchik, us Tashkent	UZ-7	41.262	69.375	444	Stream	17	19.8	8.1	420	5.14	0.200	27	8.7	520	6.56	0.965	8.0	7.6	30	1.48	0.010
Chirchik, ds Tashkent	UZ-8	41.168	69.232	375	Stream	16	21.4	7.9	523	4.27	0.095	28	8.1	610	5.39	0.248	9.0	7.6	280	1.75	0.005
Borehole near Yangiyul	UZ-9	41.094	69.053	344	ground (urban)	5	20.2	7.4	876	5.57	0.396	23	7.6	950	5.80	0.780	14.0	7.4	810	5.33	0.011
Chirchik, near inflow to Syr Darya	UZ-10	40.900	68.709	253	Stream	15	21.9	8.0	842	2.08	0.295	28	8.3	1140	3.93	2.670	10.0	7.8	500	0.48	0.001
Maykhura	TJ-1	39.027	68.785	1934	Stream	19	6.8	8.2	189	0.51	0.020	10	8.3	250	0.66	0.033	1.0	8.0	120	0.36	0.006
Varzob, gs	TJ-2	38.872	68.833	1307	Stream	19	8.0	8.1	152	0.54	0.020	12	8.6	200	0.79	0.032	1.0	8.0	110	0.32	0.009
Luchob	TJ-3	38.587	68.772	822	Stream	19	15.8	8.3	206	0.74	0.021	23	8.6	290	1.23	0.042	4.0	7.9	110	0.34	0.006
Kofarnihon	TJ-4	38.493	68.784	719	Stream	19	14.8	7.8	285	1.64	0.027	20	8.1	590	3.29	0.056	7.0	7.0	110	0.01	0.009
Drinking water facility	TJ-5	38.522	68.720	747	Ground (artesian)	19	17.6	7.2	592	6.04	0.021	22	7.7	700	6.44	0.033	13.0	7.0	180	5.14	0.006
Potable well	TJ-6	38.490	68.785	728	Ground (urban)	19	17.7	6.9	941	13.27	0.022	22	7	1140	20.40	0.045	13.0	6.4	700	7.59	0.006

383

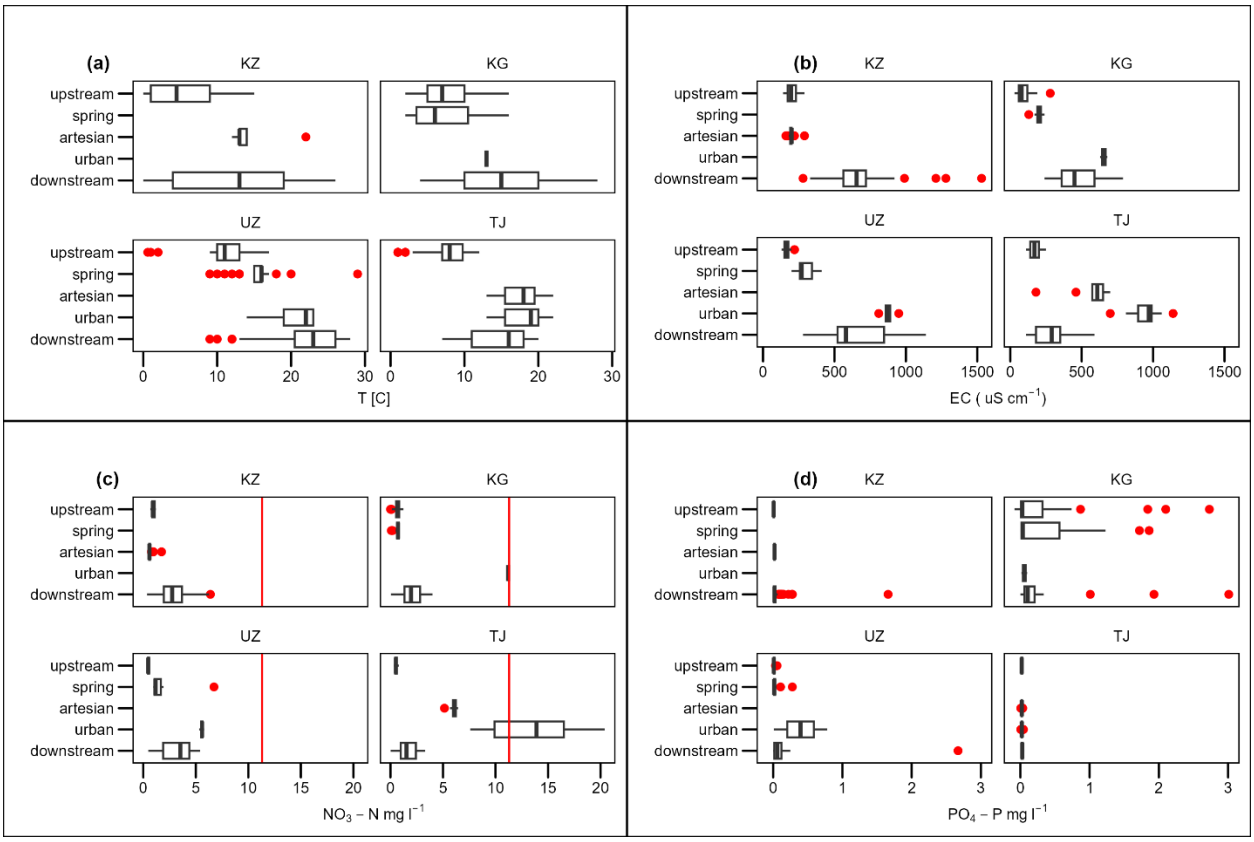

Fig. 6. Surface and groundwater water quality: (a) water temperature, (b) EC, (c) NO_3-N and d) PO_4-P upstream and downstream of urban areas, and in urban springs (springs), artesian boreholes (artesian) and urban wells (urban). The red vertical line in panel c shows the drinking water limit of 11.3 mg N l^{-1} adopted by the World Health Organization.

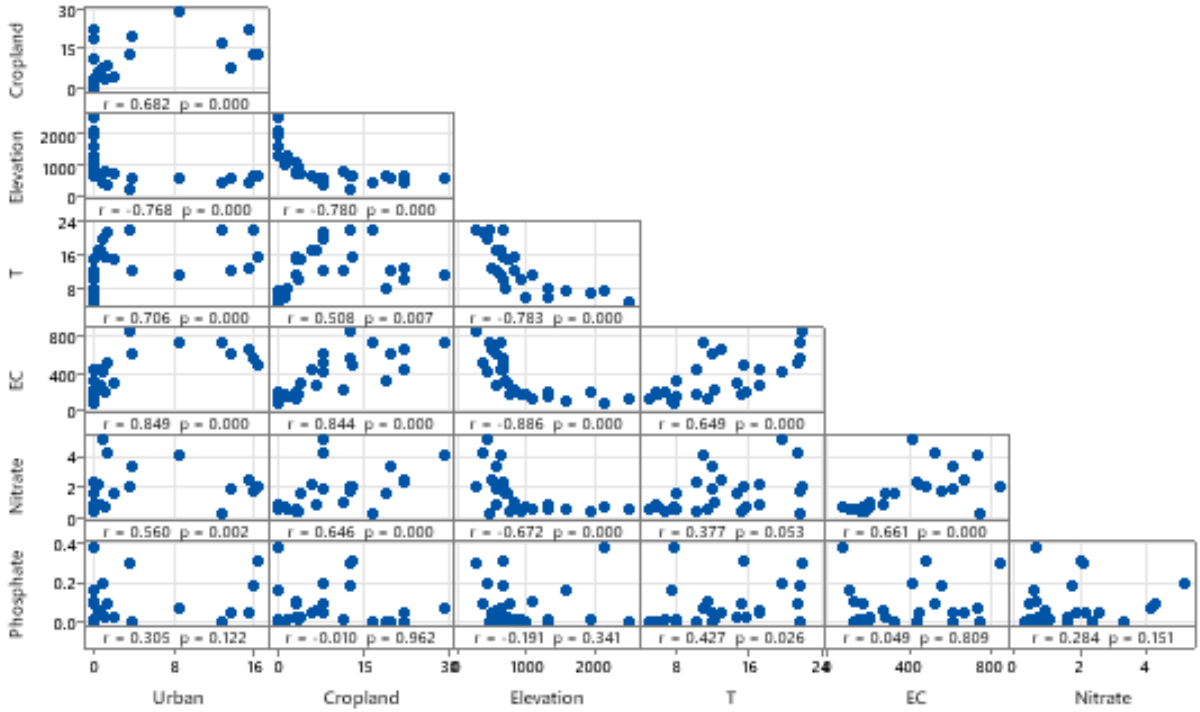

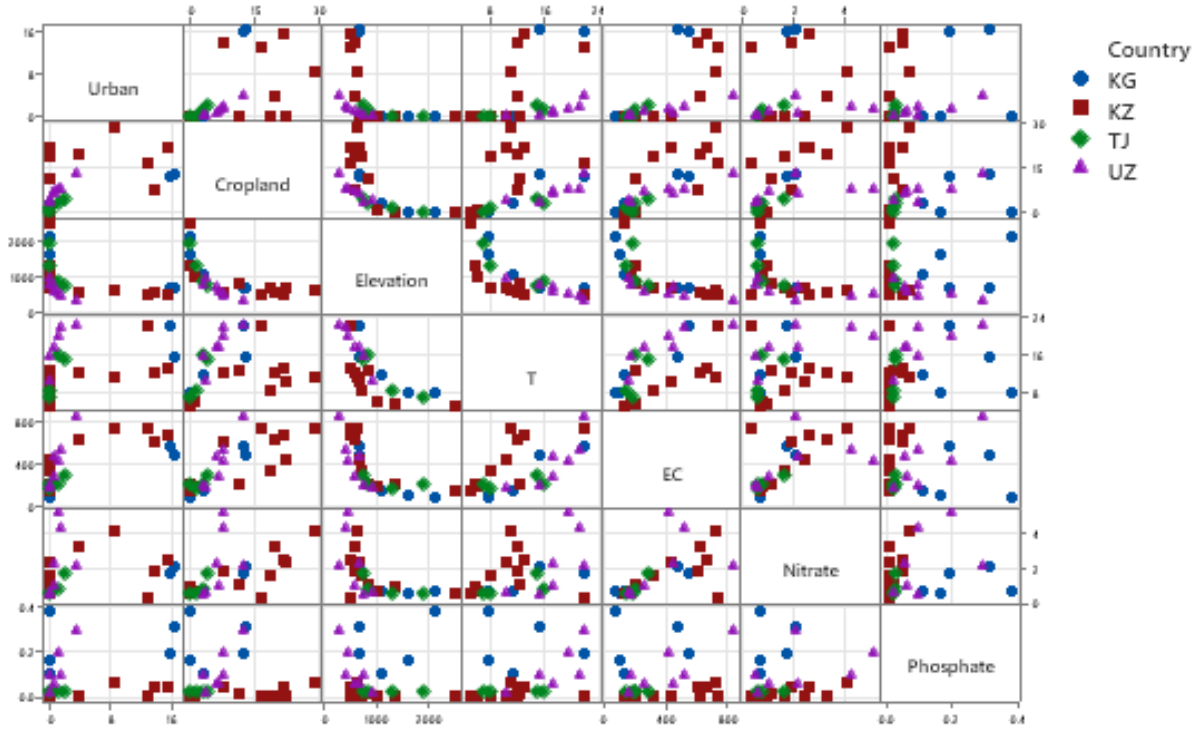

Fig. 7. Matrix scatterplot of (a) mean water quality values across all four catchments with Spearman's correlation co-efficient values and p-values shown, and (b) the same data grouped by catchment. The units are urban and cropland (% catchment area), elevation (m.a.s.l), mean air temperature (T, °C), mean electrical conductivity (EC, µS cm^{-1}), mean nitrate (mg N l^{-1}), and mean phosphate (mg P l^{-1}).

4.2. Spatial variations in surface water and groundwater quality

Along all the rivers, the predominant land cover changes from barren, mountain terrain to alpine grassland and forest and then to cropland and dry grassland steppe (Fig. 1, Table S1). In the Ala-Archa, Bishkek is located on the steppe, downstream of cropland. The Kaskelen is different as Almaty is located at the mountain base and upstream of the cropland and steppe, whilst Tashkent in the Chirchik and Dushanbe in the Kofarnihon are surrounded by cropland. The pH data show little variation either between stream water sites or with season and are generally within the range 7 to 8.6 (Table 3) suggesting any pH differences between cryosphere sources are eliminated as waters mix. There are two notable outliers. The first is the Kapshagay reservoir where the pH reaches 9, likely due to the wash-in of catchment soils enriched in calcium carbonate and bicarbonate. The second outlier is an urban well in Dushanbe where the pH is slightly acidic with a minimum pH of 6.4 most likely reflecting a more acidic geology.

4.2.1 Water temperature

The mean stream water temperature increased downstream in all catchments moving from the glaciers to the plains, reflecting the decreasing influence of glacial meltwater and the increasing air temperatures at lower elevations (Figs. 4a, 6 and S2, Table 3). Immediately downstream of the glaciers, in the Kaskelen, Ala-Archa and Kofarnihon catchments, the mean water temperatures were approximately 5 - 7 ^{o}C and the water temperature remained in this range in these catchments until the forest and alpine grassland transition to cropland and steppe when the water temperatures increased markedly in the Ala-Archa, Kaskelen and Kofarnihon. In Kaskelen and Ala-Archa, the urban groundwater temperatures were in a similar range to the surface water temperatures with a mean of approximately 13 ^{o}C indicative of groundwater and surface water mixing (Figs. 3a and 5). In Tashkent and downstream, the surface water and groundwater temperatures of the Chirchik were similar, but higher (median *c.* 22 ^{o}C), again indicative of surface-subsurface mixing.

The highest water temperatures were found in the two reservoirs, Kapshagay and Ala-Archa, with mean water temperatures of approximately 22 ^{o}C and summer maximums of 29 ^{o}C. These mean and maximum temperatures were approximately equal to those at the lowest

measurement points on Kaskelen at Arna village and Ala-Archa at the main road bridge north of Bishkek, which are immediately upstream of the reservoir inflows, demonstrating the influence of the rivers on the reservoir water quality close to the inflow. The Chirchik water temperatures were generally higher than in the other catchments because the catchment area is much larger, and the highest water quality sampling point at Mulala was further away from the glacial headwaters than elsewhere, and the lowest reaches of the Chirchik were located furthest (80 – 160 km) into the cropland and steppe.

4.2.2 Electrical conductivity (EC)

Stream water EC, a measurement of salinity, increased downstream in all catchments and was correlated with water temperature and the percentage of urban area and cropland, which all increase downstream (Figs. 4b, 6b and 7). In Kaskelen, the EC increased from approximately 130 - 200 µS cm^{-1} in Big Almaty Lake (KZ-4), a reservoir formed from a proglacial lake, to approximately 500 - 700 µS cm^{-1} downstream in the Kishi Almaty, Ulken Almaty and Kaskelen rivers and the Kapshagay reservoir (Figs. 4b and 6, Table 3). The EC measured at the upland stream water sites had a similar range to glacier melt (0 – 200 µS cm^{-1}, Section 4.1; Table 3) suggesting few additional solute inputs and instream processing until the transition from the forest and alpine grassland to cropland and steppe. High (> 800 µS cm^{-1}) EC concentrations were observed at Kosozen (KZ-8) on the Ulken Almaty, Arna on the Kaskelen (KZ-10), downstream of Bishkek on the Ala-Archa and on the Chirchik near the inflow to the Syr Darya (UZ-10), however these were lower than the World Health Organization TDS standard of 1000 mg l^{-1} (approximately equivalent to 1564 µS cm^{-1}, Yapiyev et al., 2021). Groundwater inputs to the surface water also likely increase along the continuum and groundwater has elevated EC concentrations relative to upstream surface waters due to contact time with the geology and urban pollution (Fig. S2). Thus, when groundwater enters the surface waters, this will increase the EC also, and this increase is further amplified in the lowest river reaches by evapoconcentration and soil leaching and irrigation return flow inputs. The mean EC concentrations in the Kaskelen at Arna Village and the Kapshagay reservoir were both approximately 700 µS cm^{-1} and in the Ala-Archa at the bridge and the Ala-Archa reservoir

453 approximately 500 µS cm^{-1} indicating, as for water temperature, the regulating effect of the
454 river on the reservoir water quality at least close to the inflow (Fig. 4b).

455 *4.2.3 Nitrate*

456 Mean surface-water nitrate concentrations ranged from 0 to 1.25 mg N l^{-1} at the upstream
457 stream water sites in all four study catchments and between 0 to 6 mg N l^{-1} at the sample
458 locations in, and downstream of, the major cities (Figs. 5a and 6c, Table 3, Fig. S2). Stream
459 water nitrate concentrations were correlated with EC ($r = 0.6$, $p < 0.001$) which indicates that
460 nitrate is a key component of the ion balance (Fig. 7). The greatest spatial variability was
461 observed in the Chirchik catchment with concentrations ranging from 0.5 mg N l^{-1} in the
462 headwaters (UZ-1) to over 5 mg N l^{-1} near Tashkent (UZ-7). The nitrate concentrations showed a
463 marked increase downstream of the cities in each catchment (Welch, $p < 0.0001$, Fig. S2), and
464 whilst there is a strong correlation between cropland area and stream water nitrate
465 concentration in all catchments ($r = 0.65$, $p < 0.001$, Fig. 7a), there is also a correlation between
466 nitrate concentrations and urban area ($r = 0.56$, $p < 0.01$, Fig. 7a). The highest nitrate
467 concentrations were measured in shallow well-water samples in Bishkek (approximately 11 mg
468 N l^{-1}) and Dushanbe (approximately 13 mg N l^{-1}) indicating urban groundwater pollution with
469 concentrations above the national drinking water standards of 10 mg N l^{-1} adopted in KZ, KG
470 and TJ and 9 mg N l^{-1} adopted in UZ, and the 11.3 mg N l^{-1} set by WHO (Yapiyev et al., 2021). In
471 the croplands upstream of Bishkek and Dushanbe, lower nitrate concentrations were observed
472 in springs, and an artesian well, which suggests lower pollution from farming compared to
473 urban areas (Fig. 6c). The stream water nitrate concentrations were lower than those in the
474 urban groundwater (Welch, $p < 0.0001$, Fig. S2) suggesting the groundwater contamination was
475 from urban effluent rather than the surface waters.

476 *4.2.4 Phosphate*

477 Overall, river and groundwater PO4-P concentrations are low above the urban centers, with
478 mean stream water concentrations below the detection limit of 0.05 mg P l^{-1}. Downstream of
479 the urban areas the concentrations increase to approximately 0.2 mg P l^{-1} indicating effluent
480 inputs to the lower reaches (Figs. 5b and 6d, Table 3). Very high phosphate concentrations

481 were measured throughout the Ala-Archa catchment with mean and maximum phosphate
482 concentrations of 0.38 and 2.7 mg P l^{-1} (KG-1) respectively, upstream of Bishkek, with a
483 measurement of 1.8 mg P l^{-1} in a headwater groundwater spring possibly indicating a geological
484 source (KG-2, Figs. 5b and 6d, Table 3). The corresponding EC concentrations were variable with
485 some high EC values equating to high phosphate concentrations and with some samples having
486 low EC but high phosphate. Large spikes, as high as 3 mg P l^{-1}, were also measured in the
487 phosphate concentrations in Bishkek (KG-5) which may be due to contamination by untreated
488 sewage (Figs. 1, 5b and 6d, Table 3). Relatively high phosphate concentrations of approximately
489 0.3 mg P l^{-1} were also observed in an urban well (UZ-9) in the Chirchik catchment and at the
490 surface water sampling point immediately downstream of Tashkent indicating an urban source
491 of the contamination (UZ-10; Figs. 5b and 6d, Table 3). The stream water phosphate
492 concentrations were only weakly correlated with urban area (*r = 0.3, not significant*) and not
493 correlated with cropland (*r = 0.0, not significant*), and there was little correlation with stream
494 water nitrate (*r = 0.28, not significant*), suggesting phosphate was limited in the soils and
495 stream water whilst nitrate, which is much more soluble and abundant, was leached.

4.3 Seasonal water quality dynamics

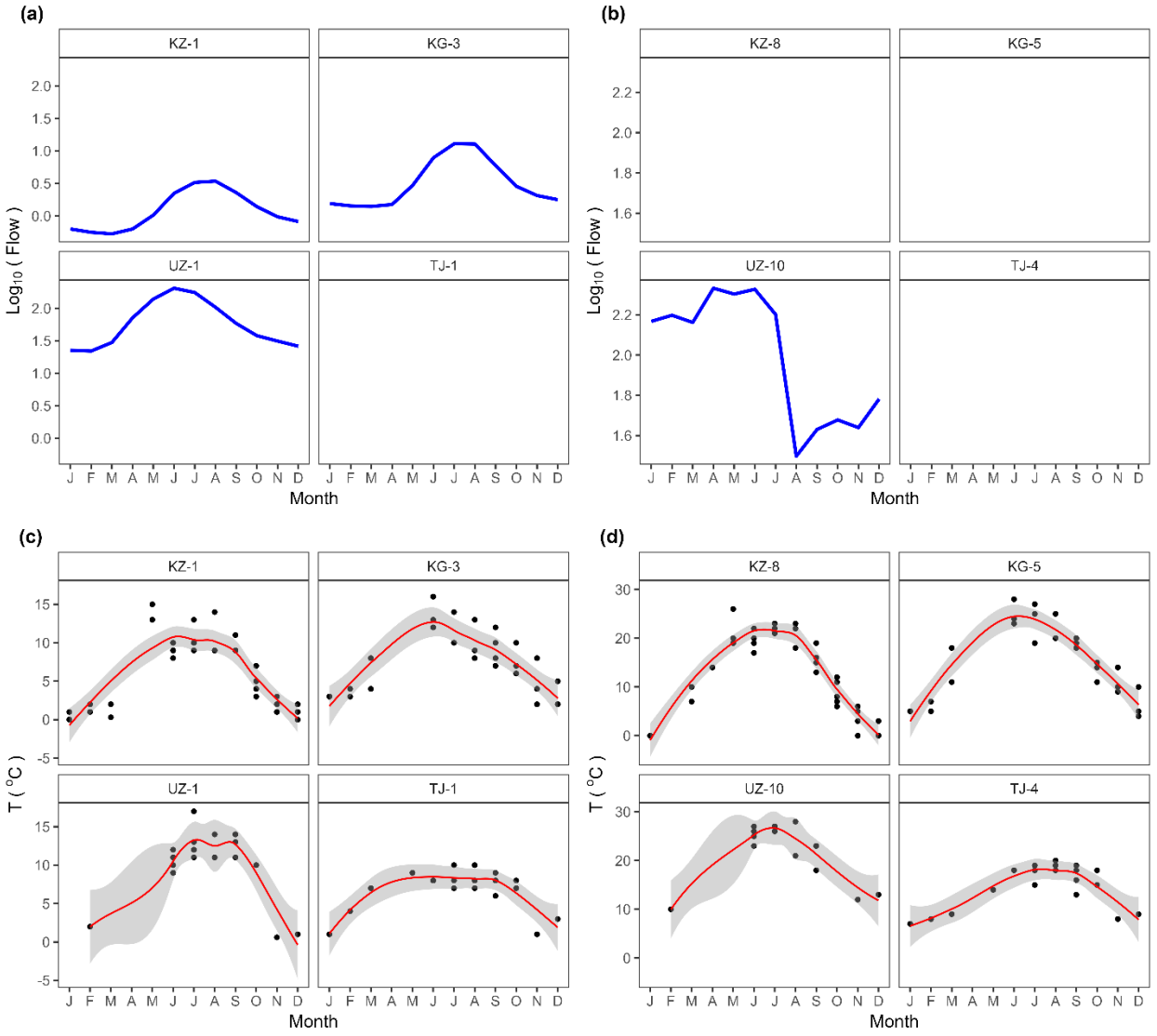

Fig. 8. Seasonal (a) Flow – high elevation, (b) Flow – low elevation (from Fig. 1), (c) Stream water temperature – high elevation, (d) Stream water temperature – low elevation in selected upstream and downstream points in each catchment (see also Fig. 1a and Table 3). The measurements were made in 2019-2020. *Continued.*

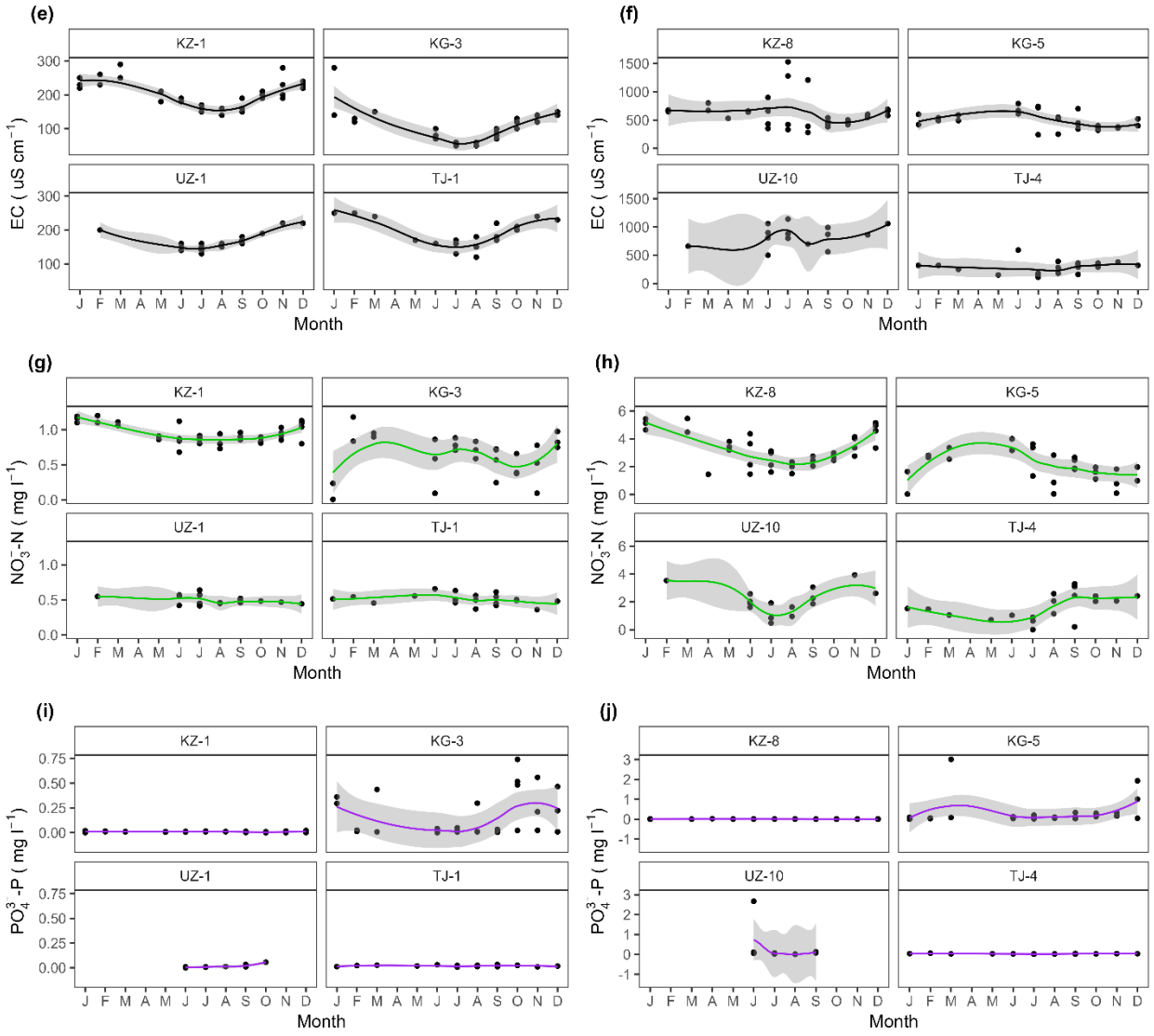

Continued from. Fig. 8. Seasonal (e) EC - high elevation, (f) EC - low elevation, (g) NO_3-N - high elevation, (h) NO_3-N – low elevation, and (i) PO_4-P – high elevation, (j) PO_4-P – low elevation in selected upstream and downstream points in each catchment (see also Fig. 1a and Table 3). The measurements were made in 2019-2020.

4.3.1 Stream flow

The seasonal variations in stream flow are described in section 2 and are drawn in Fig. 8a and 8b to allow comparison with the observed water quality dynamics. The stream measurement locations on the Kishi Almaty (KZ-1), Ala-Archa (KG-3) and Chirchik (UZ-1 and UZ-10) are co-located with stream water sampling points.

4.3.2 Water temperature

513 Stream water temperatures at the upland and lowland sites have a strong seasonal pattern
514 with temperature maximums in summer (JJA) and minimums in winter (NDJF). In the uplands of
515 the Kishi Almaty (KZ-1), Ala-Archa (KG-3) and Chirchik (UZ-1), the maximums are in the range of
516 10 to 15 ^{o}C, compared to the Maykhura River which is a headwater tributary of the Varzob
517 where the maximum is lower between 5 and 10 ^{o}C (Fig. 8b). This difference is sustained in the
518 lowland reaches with the summer stream water maximum temperatures between 20 to 30 ^{o}C
519 in the Kaskelen, Ala-Archa and Chirchik, but approximately 18 ^{o}C in the Kofarnihon perhaps
520 indicative of a greater melt water contribution.
521
522 *4.3.3 Electrical conductivity*
523 Seasonal changes in electrical conductivity (EC) were evident with EC lower under the summer
524 high flow conditions at all upstream sites suggesting solute dilution (KG-3, KZ-1, TJ-1 and UZ-1,
525 Fig. 8c and 8d). The lowest EC concentrations occurred one month after peak flow, suggesting a
526 dilution effect in the river due to the input of water with relatively low EC from glacier and
527 snow melt (see section 4.1). At the downstream-lowland locations, the meltwater inputs
528 reduced the mean EC at all sites in July and August relative to the June values commensurate
529 with an increased input of melt water (Figs. 7a and 7e). In the snowmelt dominated Kofarnihon
530 River at Dushanbe (TJ-4), the EC seasonal variation was low with a mean value of 285 µS cm^{-1}
531 demonstrating a sustained dilution even at the most downstream site below a large urban area
532 (Fig. 7b and 7f, Table 3). However, variations in EC were evident around these mean EC values
533 and in the downstream-lowlands of Ala-Archa (KG-5), the EC peaked at approximately 800 µS
534 cm^{-1} in July and August. This result demonstrates that the dilution effect on water quality can
535 be diminished downstream, but not eliminated, as the main channel becomes dominated by
536 urban and agricultural sediment and nutrient inputs. A large annual variation in EC was
537 observed at the lowest sample site on the Ulken Almaty (KZ-8), downstream of Almaty, and was
538 probably dependent on the amount of summer glacier and snow melt and altered hydrological
539 connections between soil leaching and the main river during the summer months in different
540 years. In the Ulken Almaty at Kosozen (KZ-8), the summer EC varied from 300 - 1600 µS cm^{-1} in
541 July due to differences in discharge between 2019, with high summer discharge which

associates with an EC of 300 µS cm^{-1}, and 2020 characterised by a delayed melt due to cloudy conditions and lower air temperatures resultant in lower discharge in summer, which with an EC of 1600 µS cm^{-1} (Fig. 7f).

4.3.4 Nitrate

In the Kishi Almaty (KZ-1) and Ala-Archa rivers (KG-3) at high-elevation, there is some evidence that nitrate is higher during the winter low-flow period and lower during the summer, though little seasonal variability in nitrate concentrations was observed particularly for the Chirchik (UZ-1) and Varzob (TJ-1) rivers (Fig. 8g). This suggests that the in Ala-Archa and Kishi Almaty headwaters, the nitrate flux is dominated by a steady, albeit small, supply of nitrate from the cryosphere which is diluted by summer snow melt. The cryosphere samples nitrate concentrations range from 0 to 1.2 mg N l^{-1} (section 4.1), which are close to the values observed in the upstream stream water sites. Though the concentrations are lower during the high flows in the summer, the total flux could be significant due to higher glacier melt (July-August, Fig. 2c). Further work is needed to measure flow and concentrations simultaneously. Seasonal variations in the lowland nitrate concentrations were also evident though the patterns were complex. In the lowlands, nitrate concentration peaks were observed in June and July (*c.* 4 mg N l^{-1}) in Ala-Archa (KG-5), whereas in the Kofarnihon (TJ-4) the peak occurred in September (*c.* 3 mg N l^{-1}), and in Ulken Almaty River (KZ-8) in the winter, December-March, period (c. 5 mg N l^{-1}) and there was a notable variation in nitrate concentration in June (Fig. 8h). These differences probably indicate variations in the relative inputs of nitrate from urban and cropland areas, groundwaters, the evapoconcentration effect and the timing of the meltwater input.

4.3.5 Phosphate

Both high- and low-elevation phosphate concentrations exhibited little seasonal variation (Fig. i and 8j), though concentration spikes were evident and there was some evidence for meltwater dilution or summer uptake of phosphate in the high-elevation Ala-Archa (KG-3). In the Ala-Archa River, spikes in the phosphate concentrations were measured in March (3 mg P l^{1}) and December (1.9 mg P l^{1}) at the downstream KG-5 site. The increase of phosphate at the upper site (KG-1) observed from August to November 2020 (from 1.8 to 2.7 mg P l^{-1}, respectively)

suggested some subsurface inputs to the stream water while the biggest phosphate spike in March 2020 downstream (KG-5) that reached 3.0 P l^{-1} was likely due to effluent input or possibly a deeper groundwater source (Fig. 8i). High phosphate concentrations were also measured in the Chirchik (UZ-10) in June with maximum values of 0.97 and 2.7 mg Pl^{-1} for UZ-9 and UZ-10 respectively suggesting an agricultural or urban source (Table 3, Fig. 8j). The measurements of the phosphate standards were good suggesting the phosphate spikes were real and not due to analytical error.

5. Key findings and wider implications

For the first time, an extensive spatial and temporal dataset describing key water quality parameters has been created for four glaciated catchments in Central Asia and made available. Whilst some data were available for KZ and UZ, this study extends water quality measurement to KG and TJ, increases the measurement frequency from monthly to fortnightly to better capture seasonal variations, links the cryosphere to the downstream stream water, and includes groundwater and high mountain and lowland reservoirs; all using methods common to all catchments and water types. Thus, the work begins to address recent calls for better systematic quantification of contaminants in the catchments of Central Asia through the initiation of a water quality monitoring network (Beard et al., 2022a; Beard et al., 2022b; Leng et al., 2021; Liu et al., 2021).

Our data show that nutrients can be present in significant concentrations in mountain cryosphere melt, particularly nitrate in Ulken Almaty headwaters which contained over 1 mg NO_3^--N l^{-1}. The nitrate concentrations were especially high in rock glacier and permafrost melt and the subsequent melting of these is a concern for input fluxes to downstream streams and lakes. Considering hypothesis one, the proglacial stream nitrate concentrations were found to be significantly lower than those in rock glacier melt and significantly higher than those in the snowpack melt. Given this, and the large variation in the proglacial stream nitrate concentrations, then the nitrate measured at the glacier terminus seems likely derived from a mixture of weathering and atmospheric deposition. In 1999, Vilesov and Uvarov (2001) measured elevated nitrate concentrations (up to 3. 9 mg l^{-1} of NO_3^--N) in Tyuksu glacier melt

samples, and these linked to the air pollution of Almaty from fossil fuel combustion. We did not find concentrations as high and more detailed study is required to better understand the relative contribution of nitrate to proglacial streams from weathering and atmospheric deposition, especially as air pollution of large cities in Central Asia is a growing concern (Tursumbayeva et al., 2023). The relative contributions of supraglacial, englacial and subglacial melt, including snow and firn melt, also require quantification to confirm if nitrate in CA glaciers is derived from a mix of primary and secondary sources.

Low dissolved phosphate concentrations at the high elevation sample sites suggest that the soils and stream waters were phosphorus limited with any available phosphorus rapidly assimilated by the soil or stream biota or, alternatively or in addition, that phosphorus was in a particulate form. Phosphorus can be derived from the glacier flour (Tranter, 2003) but the low phosphate concentrations in the cryosphere samples suggests that this is not an important source in the Ala-Archa. Rather the elevated concentrations may be due to small, localised sewage inputs, upstream of the sampling locations or spring water. Further measurements are required for resolution.

The water stored in upland lakes and reservoirs was clean in terms of the analytes measured and of high quality for drinking when transferred to the cities downstream. There was neither evidence of lake or reservoir acidification nor eutrophication. Based on field observations, the cold water-temperatures in the mountains, typically less than 6 ^{o}C, combined with the turbulent stream flows, appear to keep primary productivity low in streams and limited to biofilm and microbial growth, which is similar to other high mountain ecosystems (Milner et al., 2017). However, the productivity of the lakes and reservoirs requires a more complete assessment to determine eutrophication risk.

Overall, the water quality in all four catchments complied with national and World Health Organization standards along the continuum from the source to the plains. In all four catchments, there was a marked transition in water quality where the land cover changed from forest and alpine grassland to cropland, urban and grassland steppe, and there was strong evidence that land cover explained the spatial variations in the EC and nitrate concentrations

(hypothesis two). The observed longitudinal variations in stream water nitrate and phosphate concentrations were found to be similar to previous studies, being very low close to the glaciers, and higher in urban and cropland areas (< 0.23 to 6 mg N l^{-1}; < 0.05 to 3 mg P l^{-1}) (Leng et al., 2021; Yapiyev et al., 2021). The general increase in EC was caused by pollutant inputs from cropland and urban areas, higher evapoconcentration resultant from higher air temperatures and longer water residence times, and inflows of irrigation return water and soil leaching. Downstream of the land cover transition, contamination hotspots were also evident. The stream water EC remained within accepted standards for good quality drinking and irrigation water though higher (> 1000 µS cm^{-1}) values occurred near the river mouths, lowland reservoirs and groundwaters but still below levels that become problematic for human and livestock consumption (i.e., *c.* 2500 µS cm^{-1}). The groundwater had higher EC than the surface waters due to higher dissolved solutes and urban pollution, however it was not saline.

Whilst EC and NO_3-N concentrations were correlated, the increase in stream water NO_3-N concentrations at the land cover transition was less marked than for EC. This may reflect that nitrogen inputs from agriculture remain low even following economic recovery in the post-Soviet era, or that farms and farmland are managed to maintain a balance between nitrogen inputs and outputs. World Bank fertilizer application data suggest the former, with fertilizer-application rates generally low except in Uzbekistan which may explain the higher stream water NO_3-N concentrations observed in the Chirchik (Yapiyev et al., 2021).

The phosphate concentrations generally do not breach national drinking water standards; however, they are a concern for eutrophication in the lower river reaches with concentrations measured above nutrient thresholds for eutrophication (TP > 0.1 mg P l^{-1} and TN > 1 mg N l^{-1}) (Figs. 4b and 5, Table 3) (Bowes et al., 2012; Poikane et al., 2022). There was no evidence of surface-groundwater mixing diluting groundwater EC, nitrate and phosphate concentrations from bedrock contact (hypothesis three). Instead, the higher nitrate and phosphate (> 0.2 mg P l^{-1}) concentrations observed in urban wells indicate the contamination of urban groundwater with sewage effluent and, whilst not measured, this suggests likely microbial contamination given the lack of sewage treatment, particularly in Tashkent and Bishkek. Comparison of the

water temperature, EC and nitrate data all suggest that local contamination, by sewage, in the urban areas rather than by mixing with surface waters. Leng et al. (2021) modelled high total dissolved phosphorus inputs in urban locations from effluent discharges. There is some evidence of high phosphate concentrations in a groundwater spring in the Ala-Archa headwaters indicating a geological source.

In the mountains, seasonal dynamics in the water temperatures and EC were evident in all four catchments indicating ion dilution during the summer (JJA) melt. At the most downstream sites on the main river channels, a dilution effect is discernable with lower EC and NO_3-N concentrations during JJA (hypothesis four). However, the effect is variable and likely dependent on the wash-in of contaminants from croplands and urban groundwater and inter and intra-year variations in snow and ice melt. The meltwater dilution effect is difficult to quantify with the data collected because of the integration of sources, pathways, and instream processes including evapoconcentration, nitrification and denitrification, and further work to use water stable and nitrogen isotopes and models is recommended to quantify the melt water dilution effect along the main channel, and determine how higher air temperatures, an early melt season and greater spring precipitation will affect biogeochemical cycling and contaminant wash-in and dilution (Mueller et al., 2016). Any assessment should include the effect of lakes and reservoirs which control water release.

Given projected population growth in the region and the reliance on glacial melt water for irrigation and drinking, and transboundary contaminant transport in both the atmosphere and water then continued regional collaboration is required to maintain and expand the monitoring network established. The transport and release from snow and ice of trace organics, potentially toxic elements and radionuclides, now needs to be considered given projected increases in dust storms in the region (Nobakht et al., 2021), and such assessment should also include bioaccumulation and biomagnification assessments for lake and reservoir ecology and measurement of sediment transport and associated contamination (Liu et al., 2021). Our data showed that there is likely a substantial nitrate flux from the cryosphere given the relatively high concentrations measured, however, concurrent flow and concentration measurements are

required to determine accurate flux estimates for a range of solutes and particulates. Enhanced primary productivity depends on residence time, light and water temperature, and further work is needed to assess these in lakes and the lower river reaches to better assess eutrophication with consideration of organic nitrogen, phosphorus and carbon.

6. Conclusion

The first dataset to describe the water quality in four catchments in Central Asia in a systematic way for high and low flow conditions is presented. Overall, the water quality is good upstream and downstream of the transition point in land cover from alpine grassland and forest to cropland and steppe when compared with national and World Health Organization standards, and glacier and snow melt provide dilution to the downstream sections of the catchments. Shallow urban groundwater is contaminated by nitrate and phosphate, most probably from urban sewage, and these pollution hot spots are a primary concern given the use of groundwater for drinking in Bishkek and Dushanbe. The data provide a baseline against which to assess future changes in spatial and seasonal concentrations, and the newly established network of environmental research institutes in Kazakhstan, Kyrgyzstan, Uzbekistan and Tajikistan provides a basis for further systematic, water quality measurement across the region. Whilst a melt water dilution effect is discernable in the seasonal data even at the lowest monitoring points close to the river mouths, an exact quantification of the dilution effect is required, probably using stable water isotopes and modelling to determine the melt water contribution along the continuum and the implications of a reduced future melt water input on water quality.

Acknowledgements

This work was funded by the UK Global Challenges Research Fund: Research Network Grant 'Central Asia Research and Adaptation Water Network (CARAWAN, GCRFNGR3/1389): Characterising and Predicting Water Availability, Quality and Hazards in Glacier-fed Catchments' and a research grant 'Solutions to secure clean water in the glacier-fed catchments of Central Asia – what happens after the ice?' (SCWAI, UKRI Global Challenges Research Fund: Block

712 Grant). VY was supported by Nazarbayev University (CRP research grant 021220CRP2122) and
713 Ministry of Higher Education and Science (Grant AP19680027) during the preparation of the
714 manuscript. ZS was supported by the University of Reading International Studentship.

715

716 **Appendix A. Supporting information.**

717

718 **References**

719

720 Beard DB, Clason CC, Rangecroft S, Poniecka E, Ward KJ, Blake WH. Anthropogenic contaminants in
721 glacial environments I: Inputs and accumulation. Progress in Physical Geography-Earth and
722 Environment 2022a; 46: 630-648.
723 Beard DB, Clason CC, Rangecroft S, Poniecka E, Ward KJ, Blake WH. Anthropogenic contaminants in
724 glacial environments II: Release and downstream consequences. Progress in Physical
725 Geography-Earth and Environment 2022b; 46: 790-808.
726 Bettinetti R, Quadroni S, Galassi S, Bacchetta R, Bonardi L, Vailati G. Is meltwater from Alpine glaciers a
727 secondary DDT source for lakes? Chemosphere 2008; 73: 1027-1031.
728 Bogdal C, Schmid P, Zennegg M, Anselmetti FS, Scheringer M, Hungerbühler K. Blast from the Past:
729 Melting Glaciers as a Relevant Source for Persistent Organic Pollutants. Environmental Science &
730 Technology 2009; 43: 8173-8177.
731 Bowes MJ, Gozzard E, Johnson AC, Scarlett PM, Roberts C, Read DS, et al. Spatial and temporal changes
732 in chlorophyll-a concentrations in the River Thames basin, UK: Are phosphorus
733 concentrations beginning to limit phytoplankton biomass? Science of the Total Environment
734 2012; 426: 45-55.
735 Brahney J, Bothwell ML, Capito L, Gray CA, Null SE, Menounos B, et al. Glacier recession alters stream
736 water quality characteristics facilitating bloom formation in the benthic diatom Didymosphenia
737 geminata. Science of the Total Environment 2021; 764.
738 Chen Y, Takeuchi N, Wang F, Li Z. Characteristics of Chemical Solutes and Mineral Dust in Ice of the
739 Ablation Area of a Glacier in Tien Shan Mountains, Central Asia. Frontiers in Earth Science 2022;
740 10.
741 Colombo N, Salerno F, Gruber S, Freppaz M, Williams M, Fratianni S, et al. Review: Impacts of
742 permafrost degradation on inorganic chemistry of surface fresh water. Global and Planetary
743 Change 2018; 162: 69-83.
744 Crosa G, Froebrich J, Nikolayenko V, Stefani F, Galli P, Calamari D. Spatial and seasonal variations in the
745 water quality of the Amu Darya River (Central Asia). Water Research 2006; 40: 2237-2245.
746 Darcy JL, Schmidt SK. Nutrient limitation of microbial phototrophs on a debris-covered glacier. Soil
747 Biology and Biochemistry 2016; 95: 156-163.
748 Duethmann D, Bolch T, Farinotti D, Kriegel D, Vorogushyn S, Merz B, et al. Attribution of streamflow
749 trends in snow and glacier melt-dominated catchments of the Tarim River, Central Asia. Water
750 Resources Research 2015; 51: 4727-4750.
751 FAO/IIASA/ISRIC/ISSCAS/JRC. Harmonized World Soil Database (version 1.2). In: FAO R, Italy and IIASA,
752 Laxenburg, Austria, editor, 2012.
753 Farinotti D, Longuevergne L, Moholdt G, Duethmann D, Mölg T, Bolch T, et al. Substantial glacier mass
754 loss in the Tien Shan over the past 50 years. Nature Geoscience 2015; 8: 716-722.

Finaev A, Kobuliev Z, Shaimurodov F, RAkhimov I, Majidov T, Finaeva E. The use of isotope methods for water use supply of Dushanbe city. Izvestiya of Academy of Sciences of Tajikistan Republic 2017: 83-91.
Friedl M, Sulla-Menashe D. MCD12Q1 MODIS/Terra+Aqua Land Cover Type Yearly L3 Global 500m SIN Grid V006. 2019, distributed by NASA EOSDIS Land Processes DAAC. Accessed 2020-11-17 2019.
Gao J, Long LL, Klemd R, Qian Q, Liu DY, Xiong XM, et al. Tectonic evolution of the South Tianshan orogen and adjacent regions, NW China: geochemical and age constraints of granitoid rocks. International Journal of Earth Sciences 2009; 98: 1221-1238.
Groll M, Opp C, Kulmatov R, Ikramova M, Normatov I. Water quality, potential conflicts and solutions-an upstream-downstream analysis of the transnational Zarafshan River (Tajikistan, Uzbekistan). Environmental Earth Sciences 2015; 73: 743-763.
Hagg W, Hoelzle M, Wagner S, Mayr E, Klose Z. Glacier and runoff changes in the Rukhk catchment, upper Amu-Darya basin until 2050. Global and Planetary Change 2013; 110: 62-73.
Harris I, Osborn TJ, Jones P, Lister D. Version 4 of the CRU TS monthly high-resolution gridded multivariate climate dataset. Scientific Data 2020; 7: 1-18.
Hock R, Rasul G, Adler C, Cáceres B, Gruber S, Hirabayashi Y, et al. High Mountain Areas. In: IPCC Special Report on the Ocean and Cryosphere in a Changing Climate. The Intergovernmental Panel on Climate Change (IPCC), 2019.
Huss M, Hock R. Global-scale hydrological response to future glacier mass loss. Nature Climate Change 2018; 8: 135-140.
Jarvie HP, Smith DR, Norton LR, Edwards FK, Bowes MJ, King SM, et al. Phosphorus and nitrogen limitation and impairment of headwater streams relative to rivers in Great Britain: A national perspective on eutrophication. Science of the Total Environment 2018; 621: 849-862.
Jones BF, Deocampo DM. Geochemistry of saline lakes. Treatise on geochemistry. 5. Elsevier, 2003, pp. 393-424.
Kaser G, Grosshauser M, Marzeion B. Contribution potential of glaciers to water availability in different climate regimes. Proceedings of the National Academy of Sciences of the United States of America 2010; 107: 20223-20227.
Koronovsky N. Tectonics and Geology. In: Shahgedanova M, editor. The Physical Geography of Northen Eurasia. Oxford University Press, United States, 2003, pp. 1 - 35.
Kriegel D, Mayer C, Hagg W, Vorogushyn S, Duethmann D, Gafurov A, et al. Changes in glacierisation, climate and runoff in the second half of the 20th century in the Naryn basin, Central Asia. Global and Planetary Change 2013; 110: 51-61.
Leng PF, Zhang QY, Li FD, Kulmatov R, Wang GQ, Qiao YF, et al. Agricultural impacts drive longitudinal variations of riverine water quality of the Aral Sea basin (Amu Darya and Syr Darya Rivers), Central Asia*. Environmental Pollution 2021; 284.
Li PF, Sun M, Shu CT, Yuan C, Jiang YD, Zhang L, et al. Evolution of the Central Asian Orogenic Belt along the Siberian margin from Neoproterozoic-Early Paleozoic accretion to Devonian trench retreat and a comparison with Phanerozoic eastern Australia. Earth-Science Reviews 2019; 198.
Liu Y, Wang P, Gojenko B, Yu JJ, Wei LZ, Luo DG, et al. A review of water pollution arising from agriculture and mining activities in Central Asia: Facts, causes and effects. Environmental Pollution 2021; 291.
McCutcheon J, Lutz S, Williamson C, Cook JM, Tedstone AJ, Vanderstraeten A, et al. Mineral phosphorus drives glacier algal blooms on the Greenland Ice Sheet. Nature Communications 2021; 12: 570.
Milner AM, Khamis K, Battin TJ, Brittain JE, Barrand NE, Fureder L, et al. Glacier shrinkage driving global changes in downstream systems. Proceedings of the National Academy of Sciences of the United States of America 2017; 114: 9770-9778.

802 Miner KR, Kreutz KJ, Jain S, Campbell S, Liljedahl A. A screening-level approach to quantifying risk from
803 glacial release of organochlorine pollutants in the Alaskan Arctic. Journal of Exposure Science
804 and Environmental Epidemiology 2019; 29: 293-301.
805 Morris BL, George Darling W, Gooddy DC, Litvak RG, Neumann I, Nemaltseva EJ, et al. Assessing the
806 extent of induced leakage to an urban aquifer using environmental tracers: an example from
807 Bishkek, capital of Kyrgyzstan, Central Asia. Hydrogeology Journal 2006; 14: 225-243.
808 Mueller C, Zink M, Samaniego L, Krieg R, Merz R, Rode M, et al. Discharge Driven Nitrogen Dynamics in a
809 Mesoscale River Basin As Constrained by Stable Isotope Patterns. Environmental Science &
810 Technology 2016; 50: 9187-9196.
811 Narama C, Kääb A, Duishonakunov M, Abdrakhmatov K. Spatial variability of recent glacier area changes
812 in the Tien Shan Mountains, Central Asia, using Corona (~1970), Landsat (~2000), and ALOS
813 (~2007) satellite data. Global and Planetary Change 2010; 71: 42-54.
814 Nobakht M, Shahgedanova M, White K. New Inventory of Dust Emission Sources in Central Asia and
815 Northwestern China Derived From MODIS Imagery Using Dust Enhancement Technique. Journal
816 of Geophysical Research: Atmospheres 2021; 126: e2020JD033382.
817 Olsson O, Wegerich K, Kabilov F. Water Quantity and Quality in the Zerafshan River Basin: Only an
818 Upstream Riparian Problem? International Journal of Water Resources Development 2012; 28:
819 493-505.
820 Orlovsky L, Matsrafi O, Orlovsky N, Kouznetsov M. Sarykamysh Lake: Collector of Drainage Water – The
821 Past, the Present, and the Future. In: Zonn IS, Kostianoy AG, editors. The Turkmen Lake Altyn
822 Asyr and Water Resources in Turkmenistan. Springer Berlin Heidelberg, Berlin, Heidelberg, 2014,
823 pp. 107-140.
824 Painter TH, Skiles SM, Deems JS, Bryant AC, Landry CC. Dust radiative forcing in snow of the Upper
825 Colorado River Basin: 1. A 6 year record of energy balance, radiation, and dust concentrations.
826 Water Resources Research 2012; 48.
827 Poikane S, Kelly MG, Várbíró G, Borics G, Eros T, Hellsten S, et al. Estimating nutrient thresholds for
828 eutrophication management: Novel insights from understudied lake types. Science of the Total
829 Environment 2022; 827.
830 Severskiy I, Vilesov E, Armstrong R, Kokarev A, Kogutenko L, Usmanova Z. Changes in Glaciation of the
831 Balkhash - Alakol basin over the past decades. Annals of Glaciology 2016; 57: 382- 394.
832 Shahgedanova M, Afzal M, Hagg W, Kapitsa V, Kasatkin N, Mayr E, et al. Emptying Water Towers?
833 Impacts of Future Climate and Glacier Change on River Discharge in the Northern Tien Shan,
834 Central Asia. Water 2020; 12: 627.
835 Shahgedanova M, Afzal M, Severskiy I, Usmanova Z, Saidaliyeva Z, Kapitsa V, et al. Changes in the
836 mountain river discharge in the northern Tien Shan since the mid-20th Century: Results from the
837 analysis of a homogeneous daily streamflow data set from seven catchments. Journal of
838 Hydrology 2018; 564: 1133-1152.
839 Shannon S, Smith R, Wiltshire A, Payne T, Huss M, Betts R, et al. Global glacier volume projections under
840 high-end climate change scenarios. The Cryosphere 2019; 13: 325-350.
841 Telling J, Anesio AM, Tranter M, Irvine-Fynn T, Hodson A, Butler C, et al. Nitrogen fixation on Arctic
842 glaciers, Svalbard. Journal of Geophysical Research-Biogeosciences 2011; 116.
843 Telling J, Stibal M, Anesio AM, Tranter M, Nias I, Cook J, et al. Microbial nitrogen cycling on the
844 Greenland Ice Sheet. Biogeosciences 2012; 9: 2431-2442.
845 Tranter M. Geochemical Weathering in Glacial and Proglacial Environments. Treatise on Geochemistry
846 2003: 189-205.
847 Tursumbayeva M, Muratuly A, Baimatova N, Karaca F, Kerimray A. Cities of Central Asia: New hotspots
848 of air pollution in the world. Atmospheric Environment 2023; 309.

Van Tricht L, Huybrechts P. Modelling the historical and future evolution of six ice masses in the Tien Shan, Central Asia, using a 3D ice-flow model. The Cryosphere 2023; 17: 4463-4485.
Vilesov EN, Uvarov VN. Evolution of the Recent Glaciation in the Zailyskiy Alatau in the 20th Century. : Kazakh State University, Almaty (in Russian). 2001.
Viviroli D, Kummu M, Meybeck M, Kallio M, Wada Y. Increasing dependence of lowland populations on mountain water resources. Nature Sustainability 2020; 3: 917-+.
Wurtsbaugh WA, Miller C, Null SE, DeRose RJ, Wilcock P, Hahnenberger M, et al. Decline of the world's saline lakes. Nature Geosci 2017; advance on: 816-823.
Yapiyev V, Wade AJ, Shahgedanova M, Saidaliyeva Z, Madibekov A, Severskiy I. The hydrochemistry and water quality of glacierized catchments in Central Asia: A review of the current status and anticipated change. Journal of Hydrology-Regional Studies 2021; 38.
You XN, Li ZQ, Edwards R, Wang LX. The transport of chemical components in homogeneous snowpacks on Urumqi Glacier No. 1, eastern Tianshan Mountains, Central Asia. Journal of Arid Land 2015; 7: 612-622.